12-1-2021

Aryl Halides as Potential Components for O-Aryl-N-(9'-acridinyl)-hydroxylamines Antitumor Agents

Erin Munder
University of Northern Colorado

UNIVERSITY OF NORTHERN COLORADO

Greeley, Colorado

The Graduate School

ARYL HALIDES AS POTENTIAL COMPONENTS FOR O-ARYL-N-(9'-ACRIDINYL)-HYDROXYLAMINES ANTITUMOR AGENTS

A Thesis Submitted in Partial Fulfillment
of the Requirements for the Degree of
Master of Science

Erin Elizabeth Munder

College of Natural and Health Sciences
Department of Chemistry and Biochemistry

December 2021

This Thesis by: Erin Elizabeth Munder

Entitled: *Aryl Halides as Potential Components for O-Aryl-N-(9'-Acridinyl)-Hydroxylamines Antitumor Agents*

has been approved as meeting the requirement for the Degree of Master of Science in the College of Natural and Health Sciences in the Department of Chemistry and Biochemistry.

Accepted by the Thesis Committee:

_____
Michael D. Mosher, Pd.D.

_____
Hua Zhao, Ph.D.

_____
Murielle A. Watzky, Ph.D

Accepted by the Graduate School

_____
Jeri-Anne Lyons, Ph.D.
Dean of the Graduate School
Associate Vice President for Research

ABSTRACT

Munder, Erin Elizabeth. *Aryl Halides as Potential Components for O-Aryl-N-(9'-Acridinyl)-Hydroxylamines Antitumor Agents*. Unpublished Master of Science Thesis, University of Northern Colorado, 2021.

Acridine derivatives such as m-amsacrine (m-AMSA) are known to intercalate deoxyribonucleic acid (DNA). Their action targets the growth, function, and replication of cancer cells. Because of this, they are primarily used as anticancer and antimalaria drugs. Unfortunately, due to the low half-life m-AMSA possesses because of the ease of hydrolysis of the carbon 9-nitrogen bond (C9-N bond), large concentrations of the drug are needed to be pharmaceutically effective. This results in a large concentration of toxic aniline byproducts. To reduce the rate of hydrolysis but still maintain the binding to DNA, a modification to the m-AMSA structure was made. A series of m-AMSA derivatives with a hydroxylamine linkage between the acridine nucleus and the C9-pendant was prepared via a linear three-step synthesis. Commercially available aryl bromides were coupled with hydroxylamine using catalytic palladium. Once the resulting O-substituted hydroxylamine was hydrolyzed, the product could be coupled with 9-chloroacridine to form the target compounds. Spectroscopic methods such as Proton nuclear magnetic resonance spectroscopy (^{1}H NMR), Carbon-13 nuclear magnetic resonance spectroscopy (^{13}C-NMR), ^{1}H Correlation Spectroscopy (COSY), and heteronuclear single-quantum coherence (HSQC) were used to determine the purity and structure of each target derivative. The target derivatives will be analyzed and evaluated for their ability to bind DNA through thermal denaturation. A trial with DNA in a phosphate buffer through thermal denaturation was conducted to make a baseline for the thermal denaturation. The baseline

showed that the melting point of calf-thymus DNA in the specific phosphate buffer system ranged between 68-71°C.

TABLE OF CONTENTS

LIST OF FIGURES

LIST OF TABLES

CHAPTER I

INTRODUCTION

Cancer affects humans in a variety of detrimental ways. It has the potential to develop anywhere in the human body, such as the lungs, breast, colon, or blood. Some cancers will grow and become malignant, whereas others are benign. Those that are malignant can be harmful to human health. They are so prevalent, that malignant tumors result in approximately 600,000 deaths per year on average in the US alone (World Health Organization, 2021).

Despite there being different types of cancers, some similarities among different cancer cells do exist. Every cell in the body has a specific job, and typically as a cell wears out or becomes damaged, the cell will die, and a new cell will take its place. However, as cancerous cells begin to grow and multiply, they do so uncontrollably without ever dying. This results in overcrowding the normal working cells in the body, which makes it difficult for the body to operate as it should (Mayo Clinic, 2021).

Treating these rapidly growing malignant tumors requires a variety of different treatments. The three most common treatments include surgery, radiation, and chemotherapy. These treatments can be used as a combination or independently, depending on the type of cancer. Nevertheless, each of these treatments can have harmful side effects (Mayo Clinic, 2021).

Statistics show cancer kills roughly 9.5 million people a year worldwide. Due to the fact that the percent of deaths among the human population really hasn’t changed over the years, there has been a strong push to find new drugs and new treatments that might reduce the

mortality rate (Mayo Clinic, 2021). In fact, in the most recent years there are many advances in chemotherapy to treat and potentially cure cancer. Deoxyribonucleic Acid (DNA) binding drugs pose one of the more promising advances. For example, 4'-(9-acridinylamino) methane sulfon-*m*-anisidide (m-AMSA) is one such drug with excellent properties that might advance anticancer therapies. The drug, m-AMSA, has a fairly low half-life in the body ($t_{1/2}$ = 32 min in fresh mouse blood) due to hydrolysis of the carbon 9-nitrogen bond (C9-N bond) (Charmantray & Martelli, 2001). This means that fairly large doses are required in order to reach the effective concentration needed to treat cancer. Unfortunately, this implies that fairly large concentrations of the fragments of that hydrolysis are formed in the body. For m-AMSA, the result is a large concentration of aniline derivatives which are hepatic toxins (Charmantray & Martelli, 2001).

We envision the modification of the m-AMSA structure as a way to improve its effectiveness. The structure will be modified to reduce the rate of hydrolysis while at the same time maintaining the binding of this compound to DNA. This will result in less aniline formed during hydrolysis and a potentially better anticancer drug.

Therefore, we plan to prepare of a series of m-AMSA derivatives that have a greatly reduced rate of hydrolysis. The designed compounds will install a hydroxylamine group linking the acridine to the pendant side-chain (instead of an amino group like that found in m-AMSA). The resulting molecule will be less susceptible to hydrolysis. This will allow a smaller effective dose in patients and a smaller concentration of the hepatically toxic anilines. In fact, the product of hydrolysis of the target compounds will be a phenol that is much less toxic than an aniline. After preparation of the derivatives in this study, these compounds will be evaluated for their ability to bind DNA.

CHAPTER II

LITERATURE REVIEW

The Effects of Aminoacridine Drugs on Deoxyribonucleic Acid

For biological agents, acridine derivatives have been known as one of the most successful classes. They have found use primarily as anticancer and antimalaria drugs. The most promising molecules include m-amsacrine (m-AMSA) and nitracrine (Figure 2.2 and 2.1), both of which are 9-amino derivatives of acridine (Denny, 2002). After being identified as being able to bind to the nucleus in cells, their use as potential pharmaceutical agents was explored in detail. For example, acridine derivatives have been used as antimalaria drugs since the 1940s (Denny, 2002). Their chemical structure makes it easier to bind to DNA compared to other antimalaria drugs. They have been found to have half-maximal inhibitory concentration values (IC_{50} values) < 0.2 μM against Chloroquine-resistant strains (CQ) for malaria (Valdés, 2011). The IC_{50} values relate the concentration of a drug which inhibits the growth of an organism by 50% in controlled test tube environments (vitro). The IC_{50} values can be used to indicate the potency of a drug for comparison to other drugs (Aykul & Martinez-Hackert, 2016).

Figure 2.1

Molecular Structure of Nitracrine (Charmantray & Martelli, 2001).

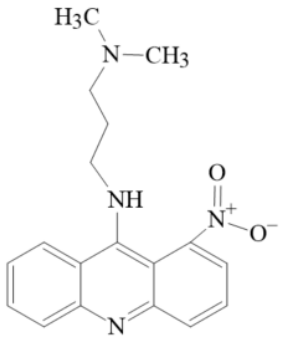

Acridines have also been considered for anticancer agents since the 1920s, but each derivatives' specific therapeutic properties like DNA intercalators are still being studied (Charmantray & Martelli, 2001). Synthetic and natural acridine drugs consists of many chemical and biological properties, some on which being DNA intercalation (Georghiou, 1977). The intercalation property in acridine derivatives result in many derivatives having a high affinity to bind with DNA. This includes acridine derivatives being able to efficient bind to DNA and disrupt the base pairs (Charmantray & Martelli, 2001).

One acridine derivative that is being studied is 4'-(9-acridinylamino) methane-sulfon-m-anisidide (m-AMSA). It binds to the base pairs of the DNA while in an equilibrium between an external association and an intercalation. While the m-AMSA is linked, there is very little structural changes that occur within the DNA (Charmantray & Martelli, 2001). When it intercalates, the DNA will lengthen, unwind, and stiffen. This will cause the DNA to have glow accessibility to transcription and translation. However, any additional hydrogen-bonding of the acridine to the DNA will increase the binding constant (Wilson et al., 1981). Derivatives of 9-Aminoacridines, such as m-AMSA, are able to intercalate DNA because they have a planar aromatic nucleus as shown in Figure 2.2 (Charmantray & Martelli, 2001). The acridine nucleus

has a unique numbering scheme, where the 9 position is immediately opposite the nitrogen. The planar nature of the system allows it to insert between adjacent base-pairs in DNA and then interact with those bases via pi-pi stacking interactions (Georghiou, 1977). If the system can also be protonated at or less than physiological conditions, the acridine nucleus will also be held in place by electrostatic interactions with the anionic phosphate backbone (Charmantray & Martelli, 2001). This is likely the case, because 9-aminoacridine has a pKa of 9.99 and 9-anilinoacridine has a pKa of 8.36 (Chavalitshewinkoon et al., 1993).

Figure 2.2

Molecular Structure of m-Amsacrine (Charmantray & Martelli, 2001).

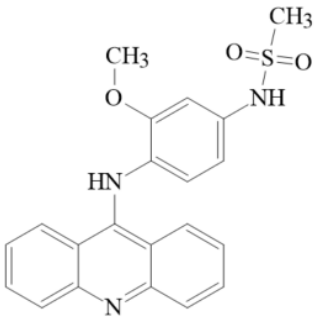

The intercalation of m-AMSA with DNA can be studied by equilibrium dialysis, spectrophotometry, or competitive binding with ethidium bromide (Wilson et al., 1981). Wilson et al. (1981) found that the binding constant was 1.0×10^5 M as well as that the intercalation events adhered to the neighboring site-exclusion principle. This principle says that the structural changes that are required to accommodate an intercalator cause the displacement of the base-pairs so much, that the adjacent potential intercalation sites are disrupted. In other words, a single acridine intercalator "ties up" three intercalation sites, the site where the intercalator is bound and the neighboring sites on either side (Wilson et al., 1981).

The drug, m-AMSA, produces side effects against tumor cells which results in interference in the DNA structure, metabolism, and inhibition of DNA synthesis. Sirajuddin et al.

(2013) found that when m-AMSA was added to calf thymus DNA, an 8 nm bathochromic shift as well as a decrease in the extinction coefficient that occurs at wavelengths above 350 nm. The drug, m-AMSA, also binds to nucleic acids at a lower affinity compared to o-AMSA (Figure 2.5) as seen in Figures 2.3 and 2.4 (Wilson et al., 1981). A bathochromic shift is the shift in absorption caused by solvent or substitution effect and results in a longer wavelength (Sirajuddin et al., 2013). These three plots correspond with the equilibrium dialysis calculated for the three derivates which m-AMSA had a low association constant of 1.3×10^5 M^{-1} compared to the association constant of AMSA at 5.5×10^5 M^{-1} and o-AMSA at 4.0×10^5 M^{-1} (Wilson et al., 1981).

Figure 2.3

The Interaction of m-Amsacrine with Nucleic Acids at 0.01 M (Wilson et al., 1981).

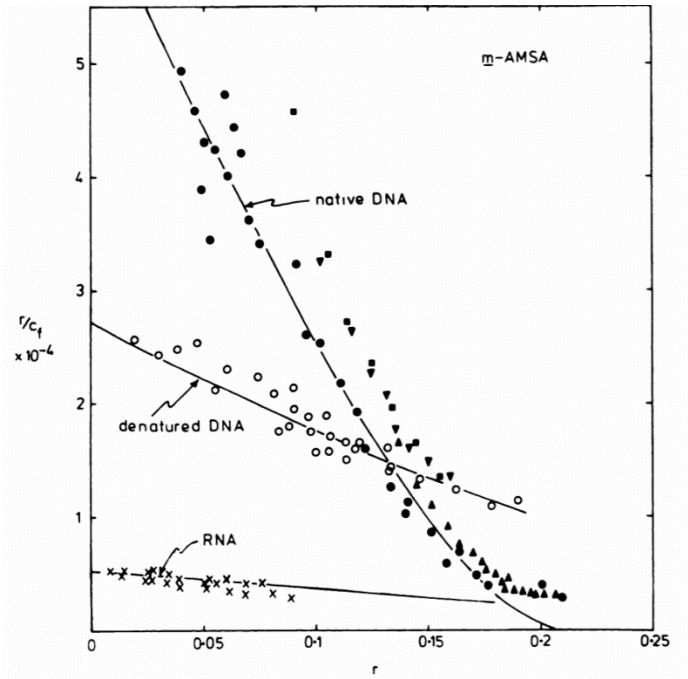

In Figure 2.3 and 2.4, is the interaction of m-AMSA (2.3) and AMSA and o-AMSA (2.4) with native (undenatured) DNA, denatured DNA, and ribonucleic acid (RNA). In both graphs, the r (x-axis) is the bound ligand per nucleotide or in other words the binding ration. C_f which is

in the y-axis in the free drug concentration. The graphs were made by equilibrium dialysis based on the interaction between the three AMSA derivatives and the nucleic acids (Wilson et al., 1981).

Figure 2.4

Amsacrine and o-Amsacrine Interaction with Nucleic Acids at 0.01 M (Wilson et al., 1981).

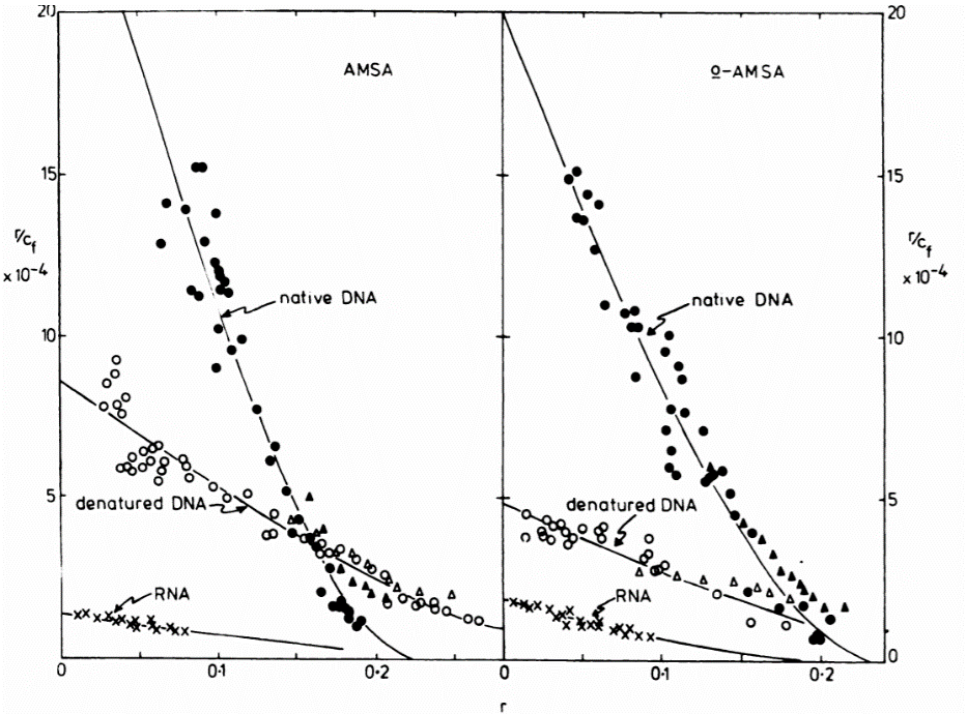

Figure 2.5

Molecular Structure of o-Amsacrine (Wadkins & Graves, 1989).

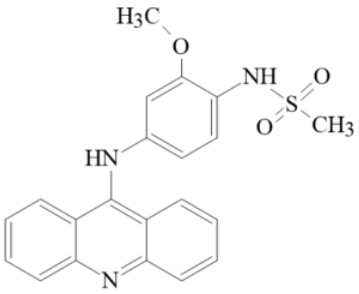

The drug, m-AMSA, has a stronger preference towards undenatured DNA as seen in Figure 2.3 and 2.4 where as AMSA and o-AMSA do not. However, all three derivatives have a higher preference toward denatured and undenatured (native) DNA than RNA (Wilson et al., 1981).

The drug, m-AMSA, has also been shown to interact with the enzyme Topoisomerase II (Topo II) (Rowe et al., 1986). This interaction inhibits the ability of Topo II to reanneal the DNA strand as it is supercoiling the DNA. An equilibrium exists between the intercalation and association of the acridine nucleus, which will result in the acridine to "walk" along the DNA strand as it is bound to the Topo II as seen in Figure 2.6 (Jang et al., 2019).

Figure 2.6

Deoxyribonucleic Acid Cleavage Reaction with Topoisomerase II Enzyme (McClendon et al., 2005).

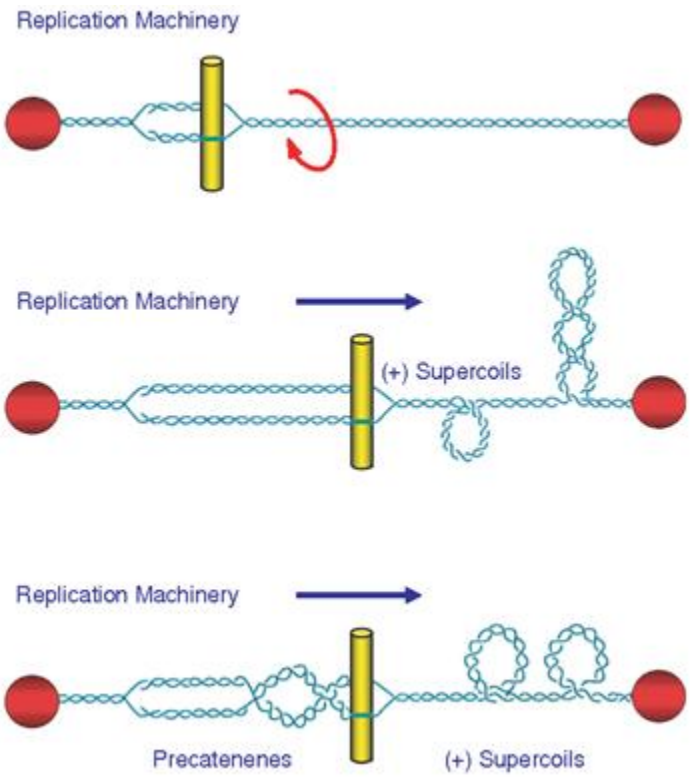

The enzyme Topoisomerase II is required for methods that require movement of a DNA strand so it can be supercoiled and ready for storage as seen in Figure 2.6. When a drug such as m-AMSA is introduced to the enzyme, the enzyme and drug will "walk" along the DNA strand creating a cleavage reaction much like the process seen in Figure 2.6. However, with the drug attached to the enzyme, the numerous breaks created along the strand will not reconnect and result in apoptosis (see Figure 2.7).

Figure 2.7

Deoxyribonucleic Acid Cleavage Reaction with Topoisomerase II Enzyme and Drug (McClendon et al., 2005).

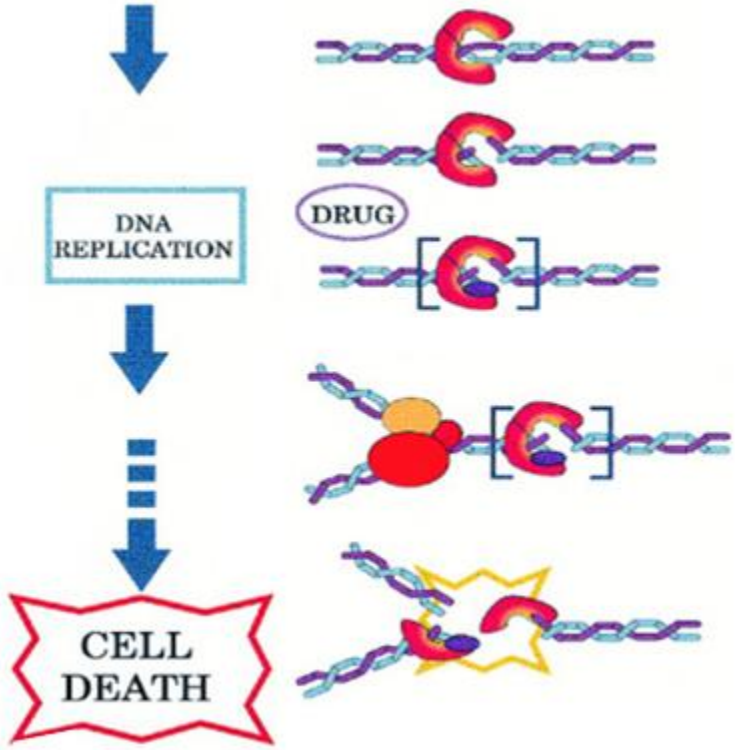

.

Thermal Denaturation of Deoxyribonucleic Acid

Deoxyribonucleic Acid is a major target for anticancer drugs. If the DNA is damaged or otherwise made unavailable, transcription and translation events are significantly impacted. A measure of the ability of a drug that targets DNA can be the reduction in the ability of DNA to go from double-stranded to single-stranded (Ageno et al., 1969). As the temperature is increased, or the pH changed, the DNA denatures to form single-stranded DNA. This process is also called "melting". The heat or change in pH is a result of a disruption of the hydrogen bonds in the base pairs (Ageno et al., 1969). As shown below in Figure 2.8, a double helical DNA strand will denature into two separate strands.

Figure 2.8

Diagram of a Double-Helical Deoxyribonucleic Acid Denaturizing (Nelson et al., 2008).

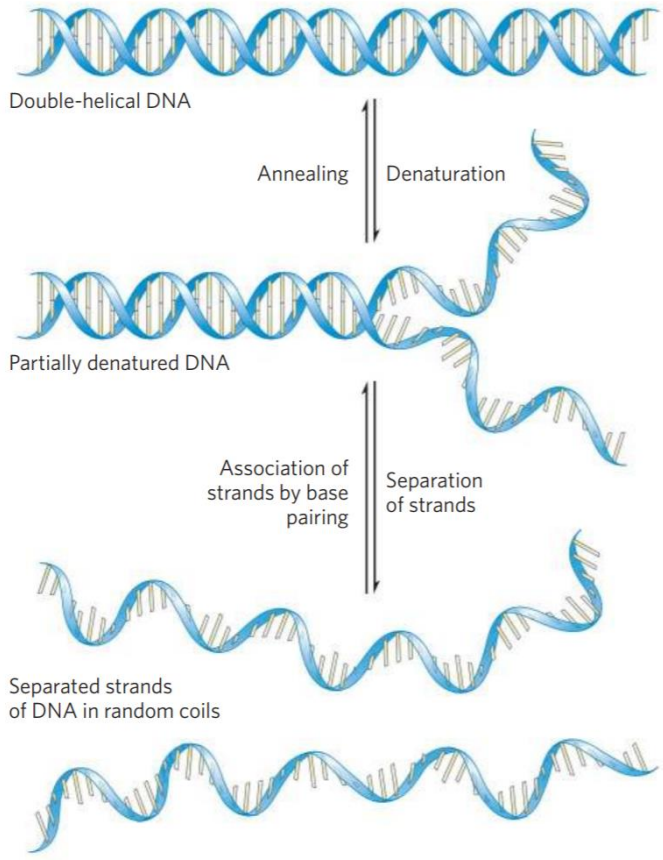

Each strand of DNA has a specific denaturation temperature (also known as the melting temperature) which will depend on the nucleotide sequence present (Ageno et al., 1969). If the DNA strand consists of more guanine (G) – cytosine (C) base pairs than adenine (A) – thymine (T) base pairs, the DNA strand will tend to have a higher melting point due to the additional hydrogen bonds that are present. Guanine-cytosine base pairs possess three-hydrogen bonds like in Figure 2.9 (Nelson et al., 2008) The additional hydrogen bond requires additional energy to dissociate. Whereas in Figure 2.8, the DNA strand consists of mainly A-T base pairs, a lower melting point will be reached which will only break the A-T base pairs and the G-C base pairs will stay intact (Nelson et al., 2008). This will result in the DNA strand partially denaturing and having bubbles present which are the broken A-T base pairs.

Figure 2.9

Diagram of a Double-Helical Deoxyribonucleic Acid Partially Denatured (Nelson et al., 2008).

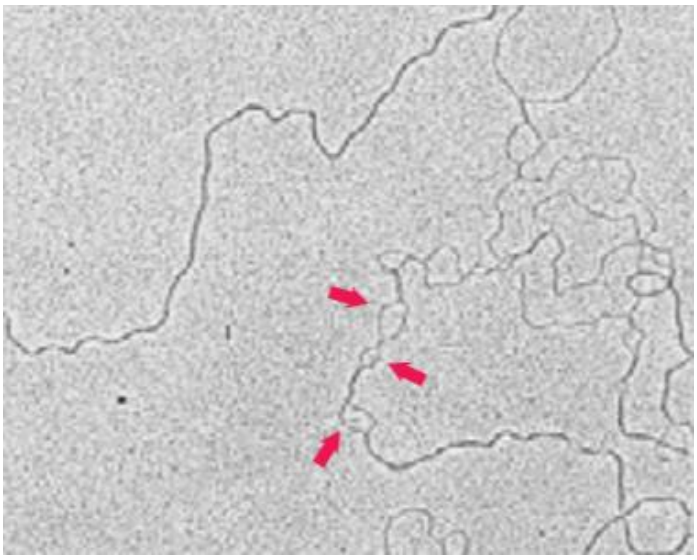

The thermal denaturation of a strand of DNA can be evaluated by plotting the absorbance of the DNA solution as a function of the temperature. This is known as a melting curve. This melting curve of DNA can characterize multiple factors of the particular DNA strand like the

physical states and the base ratio which can be taken at multiple spots on the melting curve (Russell & Holleman, 1974).

With that in mind, different concentrations of DNA can result in changes to the melting temperature of the DNA solution. Shimadzu, a Biopharmaceutical Development company, conducted a stability analysis of DNA to cross reference different concentrations to melting temperatures, which can be seen in Table 2.1. Ct(µM) is the concentration and Tm (°C) is the melting temperature.

Table 2.1

Deoxyribonucleic Acid Concentration with Corresponding Melting Temperatures (Wang et al., 2014).

Ct (µM)	Tm(°C)
196.4	62.4
157.1	61.1
117.8	60.8
98.2	59.7
78.6	58.9
19.6	55.6
15.7	54.2
11.8	53.8
7.9	52.8
5.9	51.8

To obtain the melting temperature of a DNA strand, there are multiple methods both physical and chemical in nature. The physical methods include direct probe sonication, indirect probe sonication, heating, and use of a beads mill. The chemical methods consist of using various concentrations of Sodium Hydroxide (NaOH), formamide and Dimethyl sulfoxide (DMSO) (Wang et al., 2014).

For the physical methods, the direct probe sonication was the most effective method to fully denature DNA. This method is able to disturb denatured DNA and prevent separated strands from renaturation. As seen below in Figure 2.10, direct probe sonication is the only method that showed any denaturation of the DNA. In the indirect probe sonication, the probe was outside of the centrifuge tube, unlike in direct probe sonication, which resulted in the capability of distributing the DNA decreased drastically (Wang et al., 2014). In the heating method, the heating had no effect to the DNA fragments. This could be a result of a sample size. So, as the sample was taken out of the incubator to test the denaturation efficiency, the temperature dropped resulting in renaturation occurring in the strand (Wang et al., 2014). Lastly, in the beads mill method, the glass beads not being strong enough to break the structure of the double helix in the DNA fragment.

Figure 2.10

Denaturation Efficiency by Physical Methods (Wang et al., 2014).

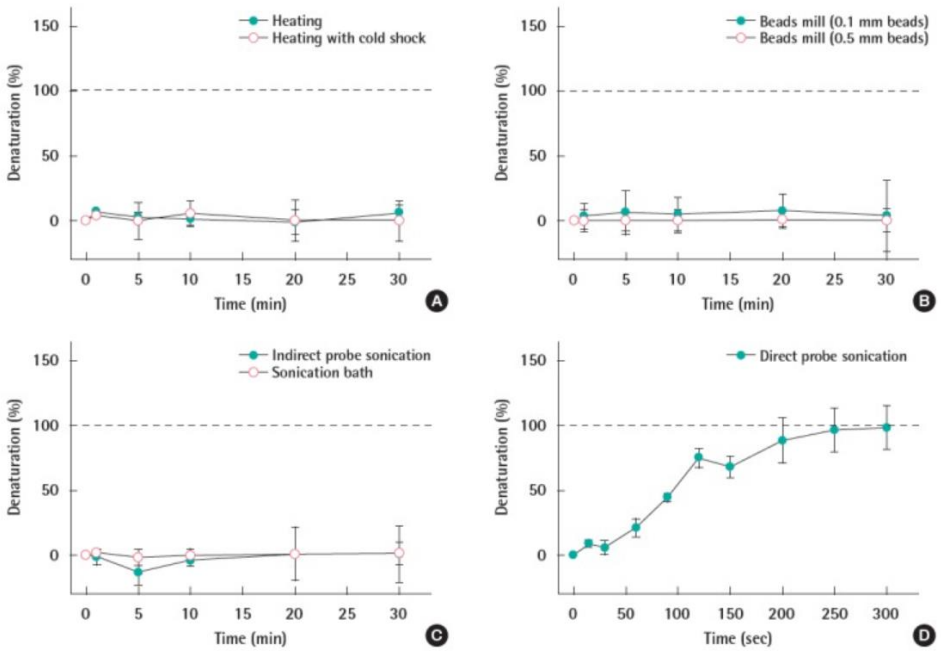

For the chemical methods, 60% DMSO and 1 M NaOH were the most effective methods for denaturing DNA. Both methods were able to fully denature the DNA fragments at a relatively fast speed. As seen in Figure 2.11, 60% DMSO and 1 M NaOH show the most denaturation of the DNA out of the three methods. The Formamide concentration were unable to denature DNA at room temperature. Other studies that used Formamide had increased the temperature to 30-36°C and had full denaturation (Blake & Delcourt, 1996).

Figure 2.11

Denaturation Efficiency by Chemical Methods (Wang et al., 2014).

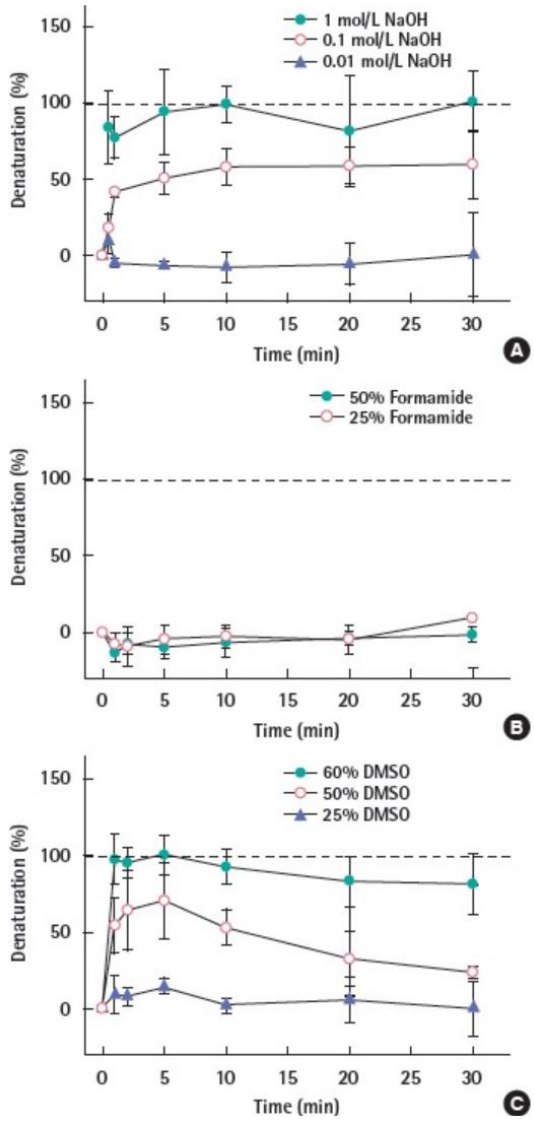

Deoxyribonucleic Acid-Acridine Binding Analyzed Using Hammett Correlations

To develop quantitative relations between different structures and activity, linear free energy relationships (LFER) can be used. One LFER method that is commonly used is the Hammett equation, which is based on the ionization of benzoic acid and its derivatives. According to Johnson (1973), the primary objective of the Hammett equation is to determine the compatibility of a substituent by comparing its effect towards the equilibrium constant of the reaction to alternative substituents. This process will clarify the inductive and resonance inputs on the free energy changes on the reaction equilibrium entirely (Johnson, 1973).

The Hammett equation can be written in many forms, but it is commonly written as

$$log\frac{k}{k_0} = \rho\sigma \quad (2.1)$$

where rho (ρ) is the reaction constant;

σ is the substituent constant;

k is the acid dissociation constant for the ionization of that specific substituent; and,

k_0 is the acid dissociation constant for the ionization of unsubstituted benzoic acid.

The sigma (σ) represents the measurement of the total polar effect utilized by the substituent that is on the reaction center (Johnson, 1973). The value is directly related to $\Delta\Delta G°$, which is the difference in free energy change for the reaction with and without that particular substituent. The Hammett equation utilizes the rates of the reaction with and without the substituent as log k and log k_0 (Bragato et al., 2020). In the original work completed by Hammett, log k refers to the rate of the ionization of a substituted benzoic acid and log k_0 symbolizes the rate of ionization of benzoic acid. These log terms are directly related to the free energy change for the two reactions: $\Delta G° = -2.303RTlogK$ (Hammett, 1937).

The magnitude of the substituent's total polar effect will depend on the orientation of the substituent on the aromatic ring in the substituted benzoic acid, as para, meta or ortho positions or σ_p, σ_m, σ_o respectively (Johnson, 1973). The specific value of σ will indicate the withdrawing or donating nature of the substituent, often referred to as the resonance and/or inductive input of the substituent. Electron withdrawing substituents have a positive σ value and electron donating substituents have a negative σ value (Bragato et al., 2020).

In the ionization of benzoic acid, electron withdrawing substituents will generate an increase in the rate of the ionization reaction related to the parent benzoic acid. This will result in the value of log (k/k_0) being greater than 1, and the value of σ for the electron withdrawing substituent is a positive value (Bragato et al., 2020). The electron density will increase at the reaction center and be absorbed by the substituent. This change will be favored by electron withdrawing substituents since it will withdraw electron density away from the reaction site itself. Substituents such as meta position chlorine (*m*-Cl), para position chlorine (*p*-Cl), meta position nitrogen dioxide (*m*-NO_2), and para position nitrogen dioxide (*p*-NO_2) are favored in this process (Bragato et al., 2020).

On the other hand, electron donating substituents generate a decrease in the ionization constant correlated to the parent benzoic acid, which is represented by log (k/k_0) and σ possessing a negative value (Bragato et al., 2020). These substituents tend to increase the electron density near the reaction site. Substituents such as *m*-alkyl groups, *p*-alkyl groups, *p*-amino groups and *p*-alkoxy groups are favored in this process as these substituents can stabilize developing cationic character at the reaction center (Bragato et al., 2020).

The Hammett equation for a single reaction will produce a straight line when the rate constants are plotted against each other. If there are multiple reactions, there could be a potential

mechanism that suggests that the reaction is subject to electronic characteristics comparable to characteristics that regulate acidity. This data can then be compared to σ values of benzoic acid series in a linear relationship to indicate whether there is a similar electron demand in the reactions or not (see Figure 2.12) (Abis et al., 1978).

Figure 2.12

Linear Relationship Plot of Rate Constants from Hammett Equation (Hammett, 1937).

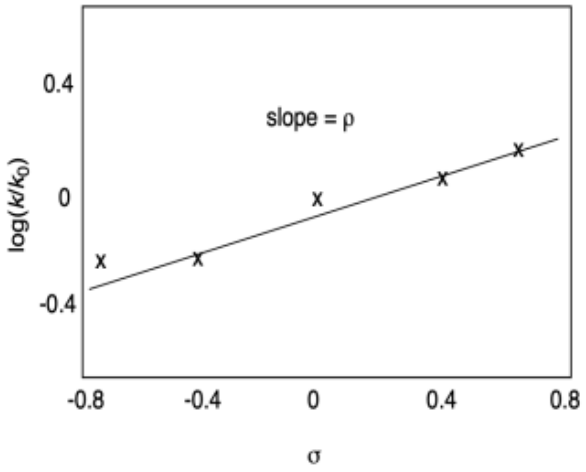

When plotting data from the Hammett equation, Rho (ρ) is the linear relationship with a proportional constant. The greater the ρ value is, the stronger the reactions depend on the electron withdrawing or donating effects (Hammett, 1937). For example, a benzoyl chloride derivative in methanol can be observed (Figure 2.13).

Figure 2.13

Benzoyl Chloride Derivative in Methanol (Hammett, 1937).

The benzoyl chloride is acting as the electrophile and the methanol is acting as the nucleophile. Since the reaction is being promoted by an electron withdrawing group and

obstructed by an electron donating group, it will follow with benzoic acid acidity and produce a positive slope in a linear relationship (Figure 2.14) (Hammett, 1937). A positive slope indicates that the reaction is dependent on the electronic factors in the same manner as the acidity of benzoic acid.

Figure 2.14

Linear Relationship Plot of a Benzoyl Chloride Derivative (Hammett, 1937).

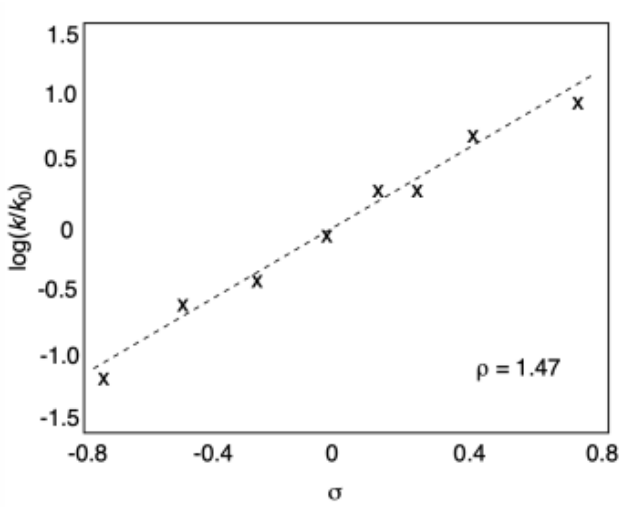

However, if an electronic withdrawing substituent in an electrophilic aromatic substitution that has a negative σ value is observed (Figure 2.16). The substituent will decrease the acidity of the reaction instead (Hammett, 1937).

The aniline derivative is acting as the nucleophile in this case (Figure 2.15). The nitrogen atom in the aniline is nucleophile and will attack the electrophilic carbonyl carbon of the benzoyl chloride (Abis et al., 1978). So, when a linear relationship is plotted, it will not follow with benzoic acid acidity and produce a negative slope (Figure 2.16). A negative slope indicates that the reaction is dependent on the electronic factors in the opposite manner as the acidity of benzoic acid (Abis et al., 1978). Furthermore, the more electron-rich the system is, the better the nucleophile and the faster the reaction is.

Figure 2.15

A Benzoyl Chloride with an Aniline Derivative (Hammett, 1937).

Figure 2.16

Linear Relationship Plot of Benzoyl Chloride with an Aniline Derivative (Hammett, 1937).

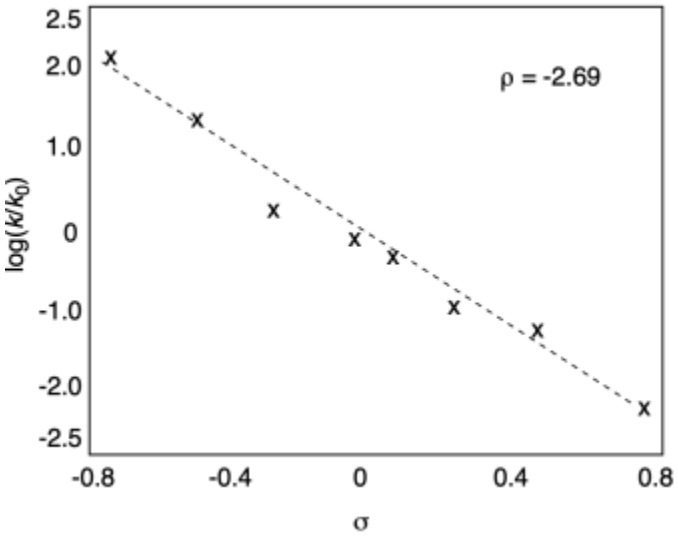

Table 2.2 illustrates various substituents and their corresponding sigma (σ) values. The σ_p indicates the substituent in the para position and σ_m refers to the substituent in the meta position. The value of σ_R represents the difference of σ_p and σ_m. While this value is not typically used in Hammett correlations, it can be used to differentiate the effects of resonance and induction of a particular substituent (Johnson, 1973).

Table 2.2

Sigma Values for Various Substituents (Johnson, 1973).

Substituent	σ_p	σ_m	σ_R
$N(CH_3)_2$	-0.83	-0.21	-0.62
OCH_3	-0.27	0.12	-0.39
CH_3	-0.17	-0.07	-0.10
H	0.00	0.00	0.00
F	0.06	0.34	-0.28
Cl	0.23	0.37	-0.14
$CO_2CH2CH3$	0.45	0.37	0.08
$CH_3C{=}O$	0.50	0.38	0.12
NO_2	0.78	0.71	0.07
$N(CH_3)_3^+$	0.82	0.88	0.06

To apply the Hammett equation to a given set of substituents from a reaction, the substituent constants (σ) and rate of reaction can be used to evaluate the type and magnitude of the charge developed in the reaction center of the rate determining step (Johnson, 1973). Which can be determined by plotting log (k/k_0) versus σ and ρ is represented by the slope of the linear plot.

The reaction in Figure 2.17 is an elimination reaction where a proton and the nosylate group (-ONs) are being eliminated and C-N π bond is created in its place (Abis et al., 1978). Overall, this is a second order reaction with a first order reaction in the substrate and base, which was determined by the following rate constants measured for various substituted constants (Table 2.3). The rate reaction (log k) and substituent constant (σ) values in Table 2.3 were plotted and presented a linear plot. The linearity of the plot Figure 2.18 supports that the substituent constants (σ) determined for the ionization of the benzoic acids are accurately modeling the electronic changes occurring in the reaction center of the rate determining center.

Figure 2.17

Elimination Reaction (Abis et al., 1978).

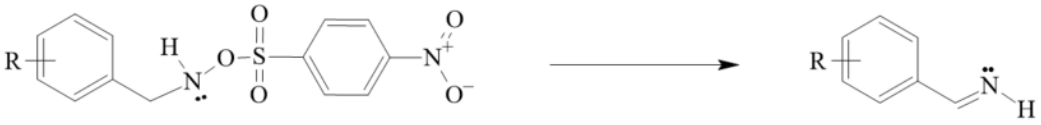

Table 2.3

Various Substituents with Corresponding Rate Constants (Abis et al., 1978).

Substituent	Log k	σ
4-CH_3	7.39 x 10^{-3}	-0.17
3-CH_3	7.94 x 10^{-3}	-0.07
H	8.69 x 10^{-3}	0
4-Cl	1.17 x 10^{-2}	0.23
3-Cl	1.50 x 10^{-2}	0.37
3-CF_3	1.54 x 10^{-2}	0.46

Figure 2.18

Hammett Plot of Rate Reactions Versus Substituent Constants for an Elimination Reaction (Abis et al., 1978)

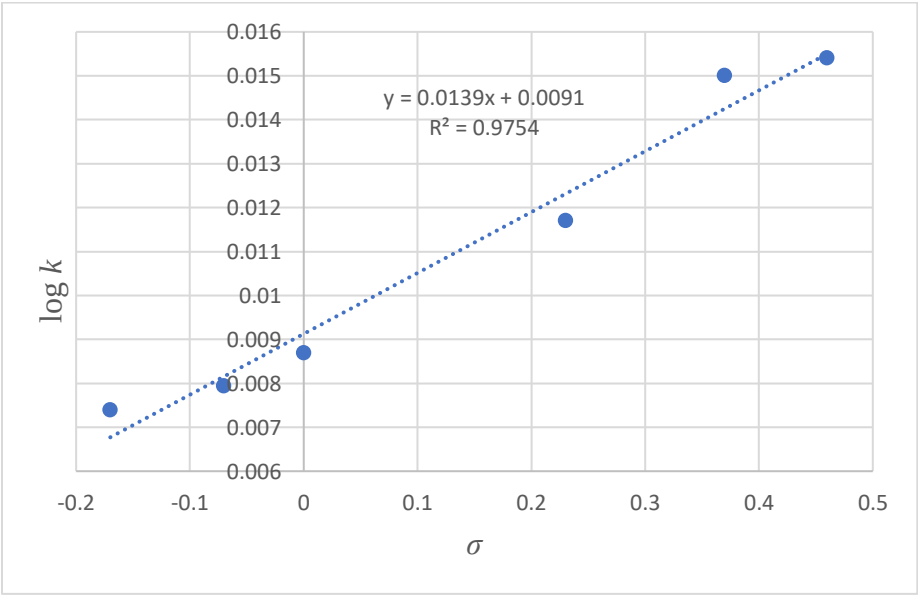

The sign and magnitude of ρ determined by the Hammett plot in Figure 2.18, indicated by y in the graph, describes the charge development at the transition state. The sign of ρ will indicate if a positive or negative charge in being developed in the reaction center of the rate determining step. A positive ρ value will indicate that the electron density in the reaction center is increase whereas a negative ρ value indicates that the electron density is decreasing. The magnitude of ρ specifies the influence a substituent will have on the reaction. Generally, values of ρ will be between 0-3 but larger values than 3 have been seen for ρ. So, a large ρ value like 4 implies the substituent influences the rate greatly and the amount of charge at the reaction center is large. In Figure 2.18, ρ is 0.057 so the substituents in Table 2.3 have a small influence on the reaction in Figure 2.17 and a partial negative charge is being formed at the reaction center of the rate determining step.

Looking at Hammett constant correlations from a biological standpoint, DNA binding constants have been found to correlate with electronic and steric parameters (Hansch et al., 2001). Specifically for 3-X-5-Y-amsacrine derivatives (Figure 2.19), specific positions for substituents on the amsacrine derivatives have been found to enhance the DNA-binding affinity (Denny et al., 1983).

Figure 2.19

Molecular Structure of 3-X-5-Y-Amsacrine (Denny et al., 1983).

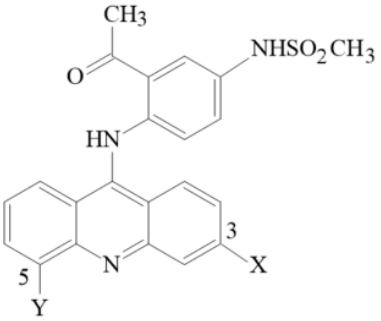

The two positions at the 3rd and 5th position in Figure 2.19 were seen to enhance the DNA binding affinity the best with the various substituents in Table 2.3. Despite the fact that the DNA-binding affinity of 3-X-5-Y-amsacrine derivatives are structure specific by nature (Denny et al., 1983).

CHAPTER III

METHODOLOGY

General Methods

All spectroscopic analyses were performed using Bruker Avance II (400MHz) multi-nuclear NMR and Thermo Fisher Scientific Nicolet iS5 FTIR Spectrometer. All chemicals were purchased from Sigma Aldrich Chemical Company or Fisher Scientific and used without further purification. Solvents were purchased from Pharmco-Aaper. To begin the multi-step synthesis, seven aryl bromides (**1a-g**) were selected and commercially purchased (Table 3.1). O-phenylhydroxylamine hydrochloride (**6h)** was previously purchased and was incorporated into the synthesis to observe how a O-aryl-N-(9'-acridinyl)hydroxylamine derivative with no substituent on the aromatic ring would react to the DNA analysis.

Table 3.1

*The Substituted Aryl Bromides (**1a-g**) and O-Phenylhydroxylamine hydrochloride (**6h**)*

Compound	R
1a	2-OCH_3
1b	3-OCH_3
1c	4-OCH_3
1d	4-$N(CH_3)_2$
1e	4-Cl
1f	4-F
1g	4-CH_2Ch_3
6h	-H

The aryl bromides (**1a-g**): 4-Bromoansiole (4-OCH_3), 3-bromoansiole (3-OCH_3), 2-bromoansiole (2-OCH_3), 1-bromo-4-chlorobenzene (4-Cl), 1-bromo-4-fluorobenzene (4-F), 4-bromo-N, N-dimethylaniline (4-$N(CH_3)_2$), 1-bromo-4-ethylbenzene (4-CH_2CH_3), anhydrous toluene, solid phenol, t-butylbrettphos (**4**) and cesium carbonate were stored at room temperature. Allylpalladium (II) chloride dimer ($(allylPdCl)_2$) (**3)**, O-phenylhydroxylamine hydrochloride, and ethyl acetohydroxamate (**2)** were stored in the refrigerator and warmed to room temperature before use. The 9-Chloroacridine (**7**) was stored in the freezer and warmed to room temperature before use.

All the glassware used in the following reactions were thoroughly cleaned with soap and water, rinsed with acetone, and further cleaned using a base bath. The glassware was also dried in the oven for at least 24 hours before use. This is to insure there was no water present in the reactions. To confirm the identity of the products of the reactions, thin layer chromatography and spectroscopic methods were used. Thin layer chromatography was performed on glass-backed silica gel with indicator plates. For the spectroscopy methods, the NMR tubes were cleaned with water and soap first then rinsed with water and acetone before being dried upside down on top of the oven for a minimum of 24 hours before use.

Each product of the reactions was isolated and purified using a Harrison Associates Chromatotron. Both 2mm and 1mm plates containing silica gel with added gypsum and fluorescent indicator were prepared. The plates were eluted with ethyl acetate and methanol and then dried on top of the oven (where the temperature was approximately 30°C) for at least 24 hours before each use. Individual compounds were isolated from reaction mixtures by collecting multiple fractions and the identity of the isolated compounds determined using the previously described spectroscopic methods.

Synthesis of Target Compounds

The synthesis of a series of O-aryl-N-(9'-acridinyl)hydroxylamines (**8a-h**) was planned to occur via a multi-step synthesis (Figure 3.1). The synthesis of each derivative was linear and begun with a specific aryl bromide (**1a-g**). Each was converted into the corresponding O-arylhydroxylamines using the method developed by Maimone and Buchwald (2010). The reaction utilizes a palladium-catalyst (**3)** and an N-protected hydroxylamine (**2**) to bypass the drawbacks with Cu-based methods, which have lower yields, long reaction times, and difficulty with substates that have ortho substituents (Maimone & Buchwald, 2010).

Figure 3.1

Multi-Step Synthesis of O-Aryl-N-(9'-acridinyl)hydroxylamines.

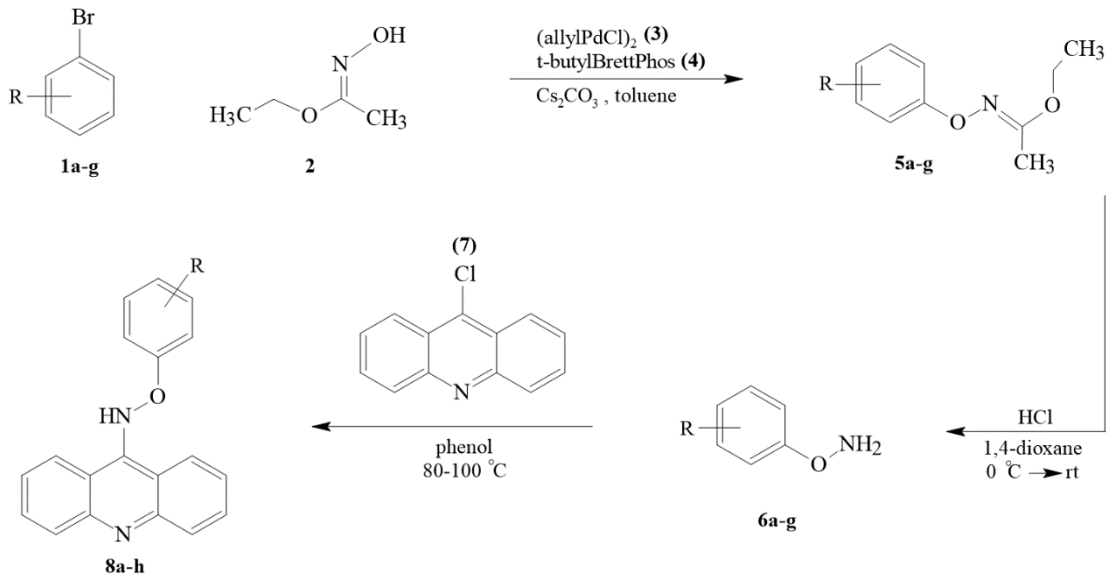

In the first step of the synthesis, (Figure 3.2) an oven dried round bottom flask was capped and cooled with argon gas to room temperature (25 °C). The argon gas was supplied to the round bottom through a needle. Once the round bottom was cooled to room temperature, the palladium catalyst ($(allylPdCl)_2$) (**3**), the ligand t-butyl brettphos (**4**, tBuBrettPhos, Figure 3.4), cesium carbonate (Cs_2CO_3) and the aryl bromide (as a solid) (**1a-g)** was added. If the aryl

bromide was a liquid, then the round bottom was completely sealed with a constant supply of argon gas before the compound is added. The addition of the aryl bromide was then followed by anhydrous toluene and ethyl N-hydroxyacetimidate (**2)**. The round bottom was then transferred to a preheated oil bath (65-68 °C) with the argon gas still present. After 1-4 hours stirring at 65-68 °C, the round bottom was removed from the oil bath and cooled to room temperature. The argon gas was not removed while the mixture was cooling. The round bottom was then rinsed with ethyl acetate and filtered through a short 1-2 cm silica gel column. The ethyl acetate was removed by the rotary evaporator before the crude product was separated on a rotary chromatography system. A crude thin layer chromatography (TLC) plate was taken before the separation. During the separation on the Chromatotron, a hexane: ethyl acetate solvent system was used. The silica gel plate in the Chromotatron was rinsed with the solvent system before the compound was placed on the plate. Individual fractions were used to collect the product (**5a-g**), which were evaluated by TLC to view the separation and compare the results to the crude TLC. The fractions containing identical compounds were combined and the solvents were removed by rotary evaporation. The identity of the product was then determined by spectroscopic methods.

Figure 3.2

Synthesis of Ethyl Acetohydroximate (Maimone & Buchwald, 2010).

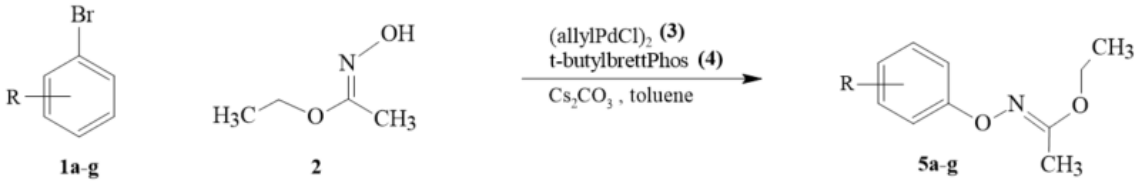

The mechanism of this organometallic reaction, as shown in Figure 3.3, begins with the oxidative addition of aryl bromide to palladium (0) (**1a-g**). The palladium (0) arises from the reduction of the original allylpalldium(II) dichloride (**3**) with the added t-butylbrettphos (**4**).

After the insertion of the palladium into the aryl-halide bond, the deprotonated the ethyl acetohydroximate (**2**) can substitute the bromide ligand on the palladium. A cis-trans isomerization will then occur before a reductive elimination that results in the product (**5a-g**) and the palladium (0) catalyst.

Figure 3.3

Proposed Mechanism of Substituted Ethyl N-phenoxyacetamidates.

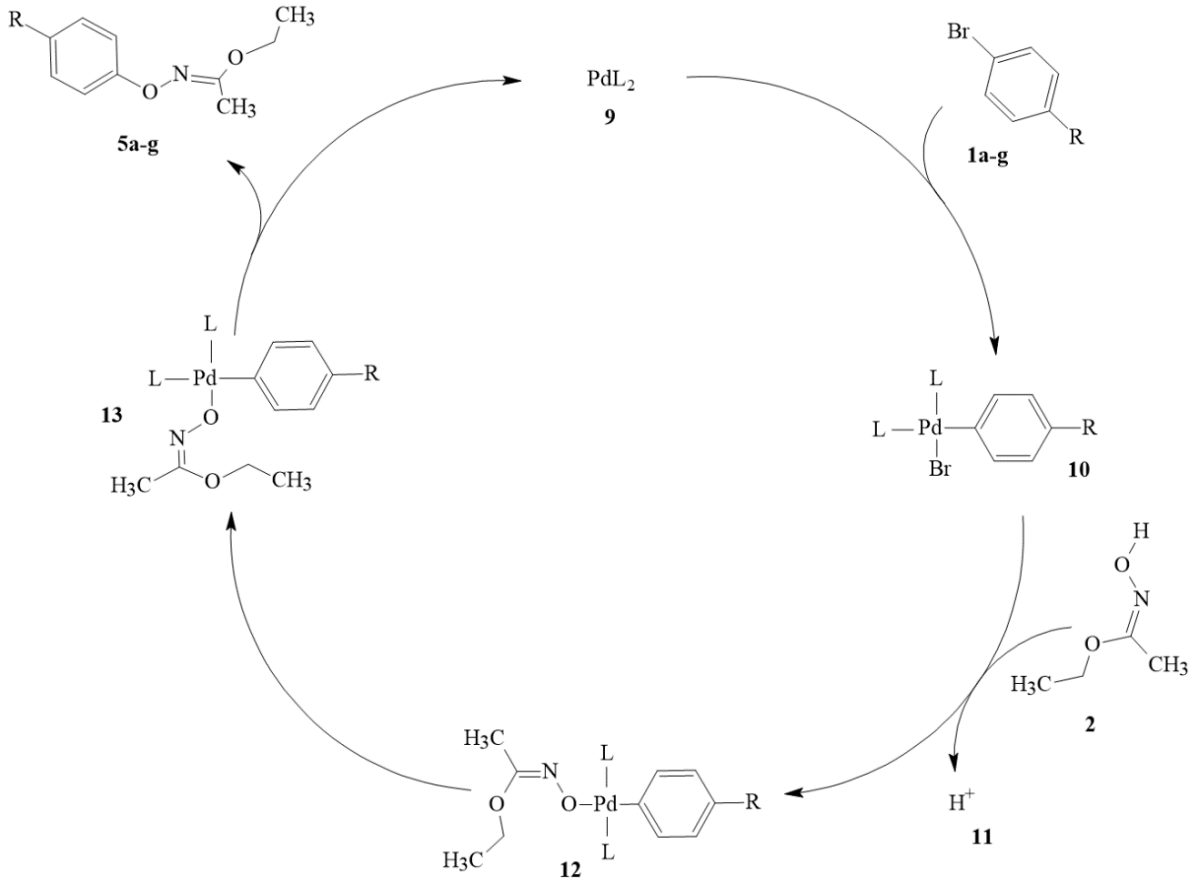

As seen in Figure 3.3, the palladium cycles from a 0 to a +2-oxidation state during the catalytic cycle. The phosphorus in the t-butylbrettphos (**4**) ligand reduces the palladium in the allylpalldium(II) dichloride (**3**) to zero so it can begin the catalytic cycle. Thus, 2 equiv of t-butylbrettphos is required for this reaction. The by-products, hydrogen (H^+) and bromine (Br^-) will be produced during the reaction. The cesium carbonate (Cs_2CO_3) will deprotonate the ethyl

acetohydroximate (**2**), creating the H^+ by-product. The deprotonated ethyl acetohydroximate will exchange with the Br^- ligand (in **9**) and completely remove the Br^- from the molecule (in **10**). The ligands specified in the mechanism are shown in Figure 3.4.

Figure 3.4

*The Molecular Structure of the tBuBrettPhos (**4**) Ligand and Palladium Complex [allylPdCl]$_2$ (**3**).*

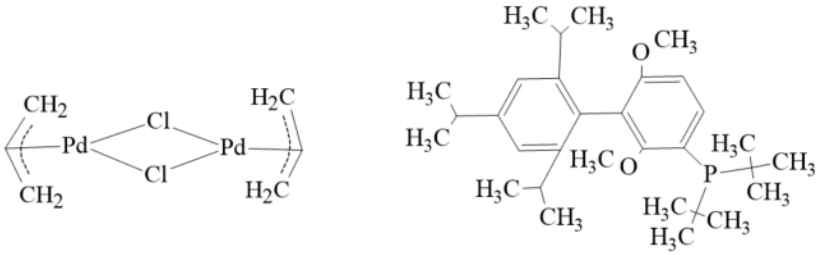

3
[allylPdCl]$_2$

4
tBuBrettPhos

For the second step of the synthesis (Figure 3.5), an oven dried round bottom containing a stir bar was completely sealed with a rubber cap and left to cool to room temperature. Then, the substituted ethyl N-phenoxyacetamidates product (**5a-g)** was dissolved in a small amount of anhydrous 1,4-dioxanes. The round bottom flask was then placed in the freezer to cool to 0 °C (10-15 mins). Once the mixture solidified, the round bottom was placed into an ice bath and uncorked so concentrated HCl could be added. Once stirred for a short time in the ice bath (5-6 minutes), the round bottom was taken out of the ice bath and stirred while the temperature warmed to room temperature over 1-4 hours. The crude product was then washed with ether and 0.01 M sodium hydroxide until a basic pH was reached. The organic phase was then washed with 0.1 M sodium hydroxide (NaOH), deionized water, and saturated brine. The rinsed product was then placed on the rotary evaporator to remove the solvent. Dichloromethane and hydrogen chloride gas were then introduced to the dried product before being vacuum filtered. The salt of the hydroxylamine was then collected and confirmed through spectroscopic methods.

Figure 3.5

Synthesis Route for the Oxime Hydrolysis (Maimone & Buchwald, 2010).

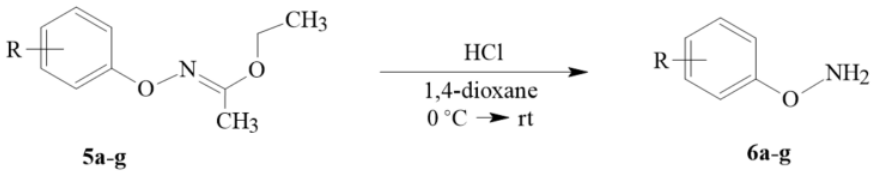

5a-g **6a-g**

The mechanism shown in Figure 3.6, where the substituted ethyl N-phenoxyacetamidate is hydrolyzed into two products: O-arylhydroxylamine (**6a-g)** and ethyl acetate (**19**). Since **6h** was commercially purchased, it was not included in the mechanism in Figure 3.6. Unlike the procedures outlined by Carlson (2015) and Forster (2020), after the hydroxylamine (**6a-g)** was made, the extraction and separation were conducted differently. Water and different concentrations of sodium hydroxide were used during the extraction process to ensure that the water-soluble compounds were completely separated from the product. Dichloromethane and hydrogen chloride gas along with vacuum filtration were used for the separation instead of the separation by rotary chromatography. This was preformed also to ensure the maximum amount of the pure product was collected without any impurities.

Figure 3.6

Proposed Mechanism of Hydrolyzed Substituted Ethyl N-phenoxyactamidates (Maimone & Buchwald, 2010).

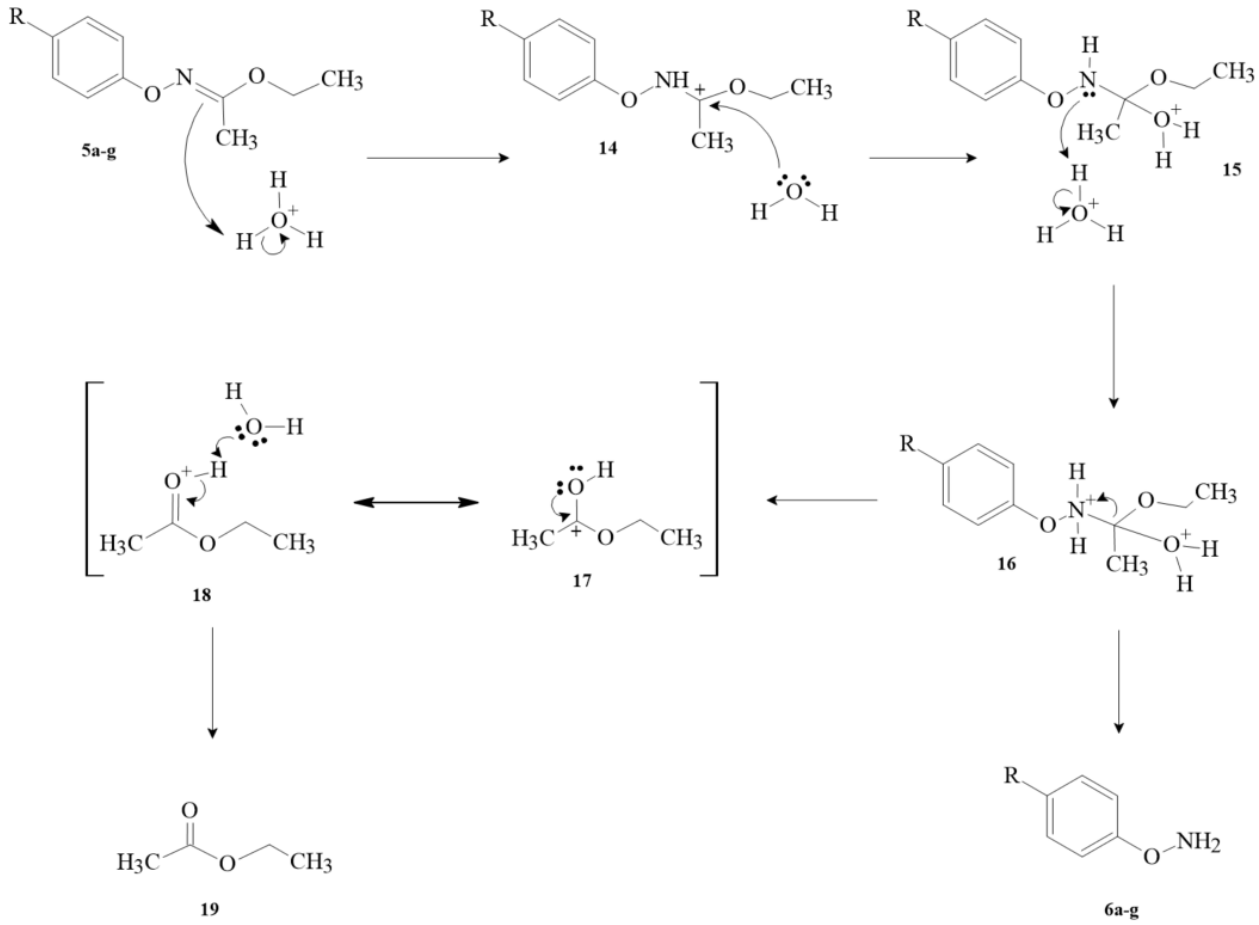

For the final step in the synthesis (Figure 3.7), the O-arylhydroxylamine (**8a-h**) was added with phenol in an oven dried round bottom containing a stir bar. The mixture was then heated. Potassium carbonate was also added to enhance the reactivity and cleave the salt of the hydroxylamine. Once the phenol melted and the temperature stabilized between 80-100 °C, 9-chloroacridine was added. The reaction was stirred for 12-15 hours at the stabilized temperature. The reaction used a 1.5:1 mole ratio of O-arylhydroxylamine to 9-chloroacridine which would make the 9-chloroacridine the limiting reactant.

Figure 3.7

Synthesis Route for the Substituted O-Aryl-N-(9'-acridinyl)hydroxylamines.

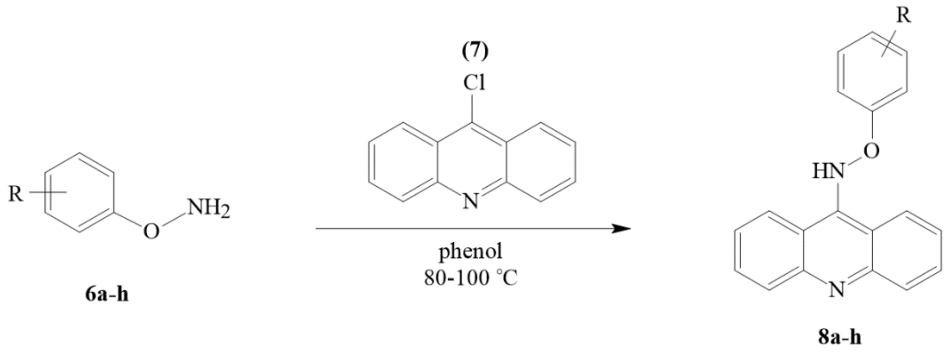

At the end of the 12–15-hour reaction time, the solution was cooled to room temperature and dissolved in dichloromethane. The mixture was then washed successively with 0.5 NaOH, D.I. water and brine. The organic product was then dried over sodium sulfate and the solvents removed by rotary evaporation. To ensure that the removal of the phenol was successful and the excessive formation of 9-hydroxyacridine was reduced a 1:1 mole ratio of phenol: sodium hydroxide was used during the washings. After the crude product was purified through a small guard column, the products were isolated by radial chromatography and identified by spectroscopic methods.

This reaction is achieved with an addition/elimination mechanism as seen in Figure 3.8. The 9-chloroacridine reacts with the phenol first since the phenol is present in significant quantities in the reaction. This interaction will form a phenoxy ion and displace the chloride (**19-21**). This is where the hydroxylamine will come in and displace the phenol since it is a good nucleophile (**23**).

Figure 3.8

Proposed Mechanism of O-Aryl-N-(9'-acridinyl)hydroxylamines (Maimone & Buchwald, 2010).

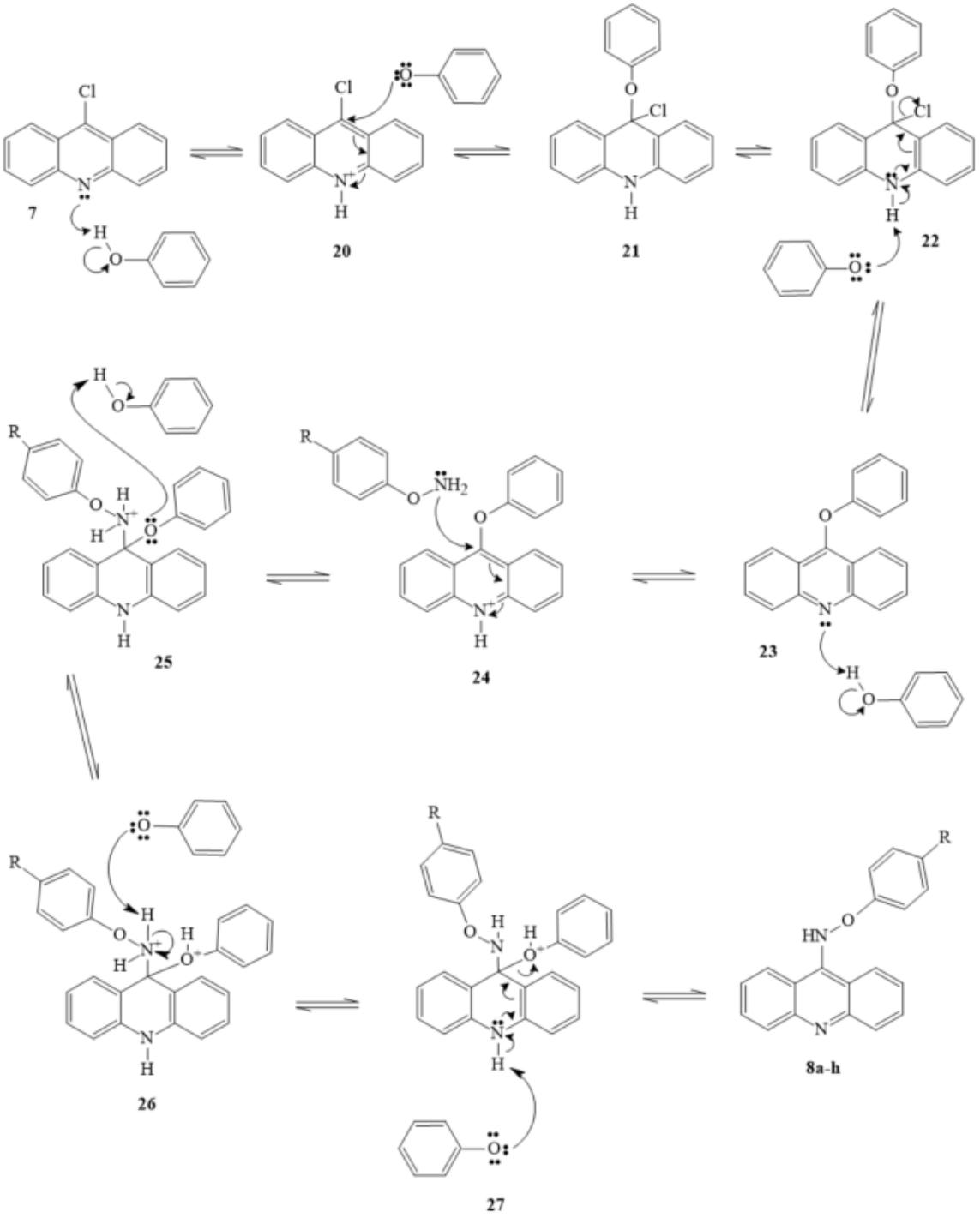

An analysis of the ability of the final compounds to bind DNA was conducted. A DNA solution was made using genomic calf thymus DNA that commercially obtained from Sigma

Aldrich. A The 0.001 M phosphate buffer at pH 6 was prepared and used to dissolve the DNA into the desired concentration using volumetric flasks. The desired concentration was determined with a pH meter and fluctuated with 0.1 M NaOH and 0.1 M hydrochloric acid (HCl) if needed. The thermal denaturation temperature, T_m, of the DNA in the solution was determined by plotting the absorbance of the solution versus a slowly increasing temperature (Carlson, 2015). The inflection point, indicating where the DNA has been 50% converted from double-stranded to single-stranded, was recorded as the thermal denaturation temperature.

The acridine derivative solutions were prepared using the compounds synthesized by the three-step process using the phosphate buffer as the solvent. The concentrations of each solution were dependent on the concentration of the DNA solution and was designed to be a 1:1 molar ratio of DNA: acridine with a final concentration of DNA set at approximately 1.0×10^{-6} M. Thermal denaturation of the DNA was then determined for each mixture of DNA and acridine compound. In cases where dimethyl sulfoxide (DMSO) was needed to ensure solubility of the acridine, the final concentration of DMSO in the DNA: acridine mixture was limited to <10%.

Finally, the measured thermal denaturation data were compiled into a quantitative-structure activity relationship. The Hammett sigma values for the different substituents was used to correlate the electronic effects of the different acridine compounds to the ability of the compounds to bind calf thymus DNA. The correlation was plotted to determine any trends in the information.

CHAPTER IV

RESULTS AND DISCUSSION

A series of O-aryl-N-(9'-acridinyl)hydroxylamines (**8a-h**) was prepared in a multi-step synthesis starting with commercially available substituted aryl bromides and O-phenylhydroxylamine hydrochloride. The multi-step synthesis began with a method developed by Maimone and Buchwald (2010). O-Phenylhydroxylamine hydrochloride was incorporated into the synthesis to observe how a O-aryl-N-(9'-acridinyl)-hydroxylamine derivative with no substituent on the aromatic ring would react to the DNA analysis. The aryl bromides (**1a-g**) and O-phenylhydroxylamine hydrochloride (**6h**) used with their corresponding Hammett Sigma values are shown in Table 4.1. The reported Hammett sigma value corresponds to either σ_o, σ_m, or σ_p depending upon whether the substituent is ortho, meta, or para.

Table 4.1

*Substituted Aryl Bromides **(1)** and O-Phenylhydroxylamine hydrochloride **(6)** with Corresponding Hammett Sigma Values.*

Compound	R	Hammett Sigma Value, σ
1a	2-OCH3	0.08
1b	3-OCH3	0.12
1c	4-OCH3	-0.27
1d	4-$N(CH_3)_2$	-0.83
1e	4-Cl	0.23
1f	4-F	0.06
1g	4-CH_2CH_3	-0.15
6h	-H	0.00

Maimone and Buchwald's method (2010) was originally developed to use relatively electron density neutral substituents such as para position cyanide (*p*-CN), para position tert-butyl (*p* -tBu), meta position dimethylamine (*m*-$N(CH_3)_2$). Their methodology showed that these substituents, formed a product with greater yield than when using strong electron withdrawing or electron donating substituents. To further investigate the theory of strong electron withdrawing and electron donating substituents having lower yields, the commercially available aryl bromides shown in Table 4.1 were chosen based upon position and the Hammett sigma value of the substituent on the aryl ring. The substituents chosen were mainly para substitution in order to determine inductive versus resonance contributions and how they relate to electronic and steric parameters of different σ magnitudes. An ortho and meta position was also selected to observe the varying effects of resonance, induction and steric hinderance from the same substituent, such as methoxy (-OCH_3).

Figure 4.1

Synthesis for the Preparation of Substituted Ethyl N-phenoxyacetamidates.

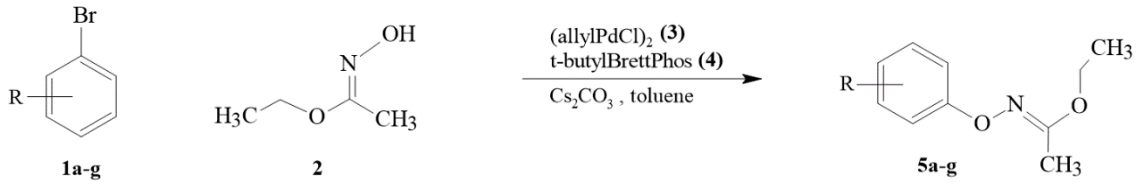

The palladium coupling reaction used to synthesize ethyl N-phenoxyacetamidates **5a-g** provided generally moderate to excellent yields. A combination of allylpalladium (II) chloride dimer (**3**), *t*-bubrettphos (**4**), cesium carbonate, and the substituted aryl bromide (if solid) (**1a-g**) was prepared under argon gas. The liquids, the substituted aryl bromide (if liquid), toluene and ethyl acetohydroxamate (**2**) were added to the reaction vessel using a syringe under inert atmosphere conditions. The sealed mixture was kept under argon gas while stirring in a heated

oil bath. The yellow-colored solution slowly turned dark red orange or dark brown color with a cream color solid on the bottom of the flask as it was heated and stirred. The crude reaction was filtered through a short silica gel column with ethyl acetate. The round bottom flask was rinsed with ethyl acetate and added to the silica gel column to ensure a quantitative transfer. The filtered product mixture was then purified through rotary chromatography. During the chromatography, the product was collected in fractions to ensure the isolation of the product. The fractions were analyzed via thin-layer chromatography and those fractions containing the same compounds combined. The products of the reaction were confirmed using ^{1}H NMR (Table 4.2) to confirm the identity of the isolated compounds.

Table 4.2

^{1}H NMR Peaks Observed for Ethyl N-phenoxyacetamidates.

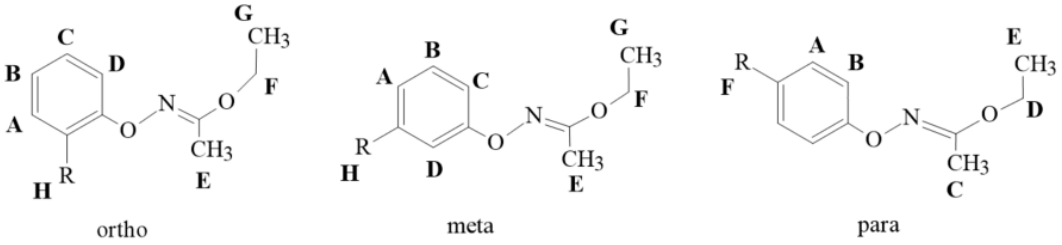

Chemical shifts of selected protons

Compound	R	A	B	C	D	E	F	G	H
5a	2-OCH_3	7.56	6.93	6.86	7.31	2.07	4.14	1.28	3.92
5b	3-OCH_3	7.22	6.74	6.55	6.77	2.13	4.24	1.37	3.82
5c	4-OCH_3	7.09	6.85	2.10	4.19	1.36	3.80	*	*
5e	4-Cl	7.26	7.10	2.13	4.20	1.37	--	*	*
5f	4-F	7.10	6.98	2.13	4.2	1.37	--	*	*

Note: "*" indicates that the signal would not be seen in the molecule. "--" indicates the signal was not present.

Maimone and Buchwald's procedure (2010) noted that the ethyl N-phenoxyacetamidates were volatile, so they were not completely evaporated to dryness using a rotary evaporator. This

was determined to not be the case with the substituents used in this study. It was determined that large amounts of solvent would still be present in the product when using the rotary evaporator for short amounts of time. Furthermore, with ethyl acetate being used to separate the products, it was crucial to fully evaporate the solvent so no ethyl acetate signals would be present in the ^{1}H NMR spectra. This was because residual ethyl acetate resonances would obscure the ethyl hydroximate signal group.

Based on Table 4.2, the R groups -Cl (**5e**) and –F (**5f**) were not seen in the ^{1}H NMR spectra, which is mainly due to ethyl acetate signals conflicting with the oxime's ethyl group. A COSY was obtained to confirm which protons corresponded to each peak (Figure 4.2).

In Figure 4.2, the green circle illustrates the correlation between the methyl proton and an aromatic proton, signal "B". The orange circle illustrates the ethyl group segment of the ethyl acetohydroximate (**5e**). The methyl proton, signal "C", correlates to the up field aromatic proton. This means signal B corresponds to the up-field signal as well since signal "B" is closer to the methyl group than signal "A". Which corresponds with the proton that is closest to chlorine since it would shift that proton's signal more downfield.

Figure 4.2

*COSY of Ethyl N-(4-chlorophenoxy)-acetamidate (**5e**) to Confirm Aromatic Protons. The Colored Circles Indicate Key Correlations in the Molecule.*

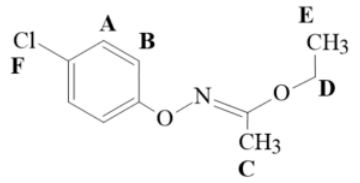

para

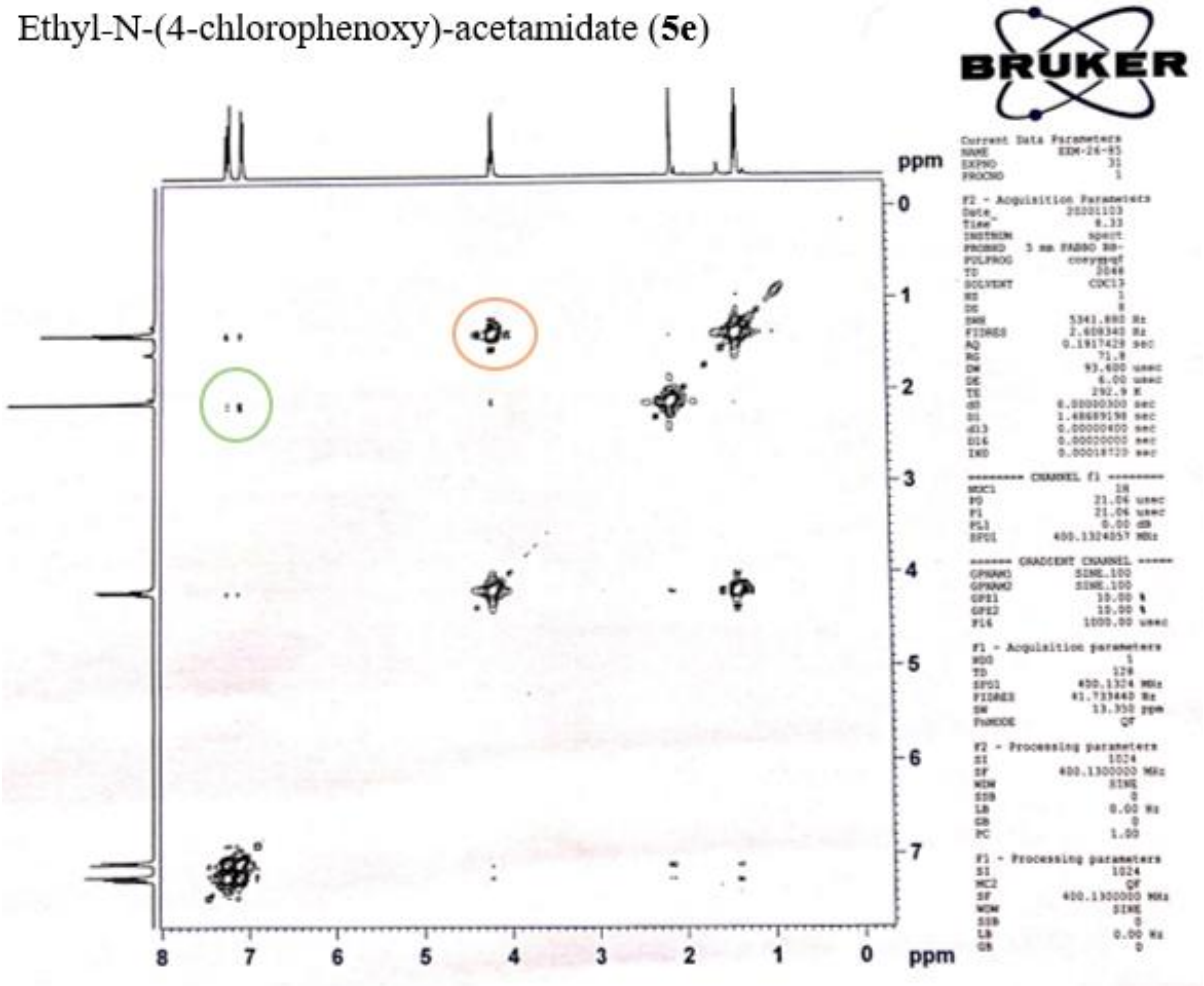

The acetamidate is known to have two diastereomers, anti and syn, due to the fixed position of the oxygen on the sp^2 nitrogen of the oxime (Figure 4.3). However, the separation process was successful in isolating the anti-diastereomer only. Forster's (2020) procedure noted the two diastereomers to have a 2:1 ratio since the syn diastereomer is less favored due to steric hindrance. That ratio was set during the preparation of the ethyl acetohydroximate that was obtained commercially. Using standard preparation reactions, the relative size of the groups on the oxime (the ethoxy vs the methyl) directly correlates to the relative ratio of diastereomers. The two diastereomers were not separated since the diastereomers displayed nearly identical R_f values during the chromatography and the next reaction would remove the diastereomeric oxime bond.

Figure 4.3

Syn and Anti-Diastereomers of Ethyl N-phenoxyacetamidates.

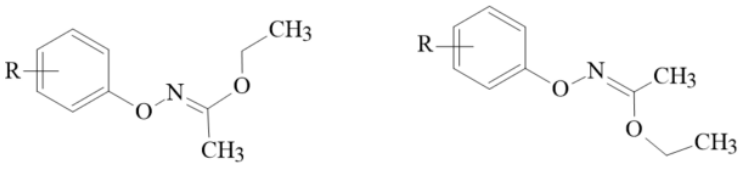

Anti-isomer Syn-isomer

The chemical shifts for ethyl N-(3-methxoyphenoxy)-acetimidate (anti diastereomer) from Table 4.2 are shown displayed in the ^1H NMR (Figure 4.4). The peak at 7.3 ppm is a solvent peak from deuterated chloroform, which was used for this proton NMR. This solvent was used since it does not cause peak exchange with compound.

Figure 4.4

*[1]H NMR of the Anti-Diastereomer of Ethyl N-(3-methxoyphenoxy)-acetamidate (**5b**).*

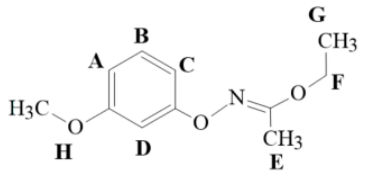

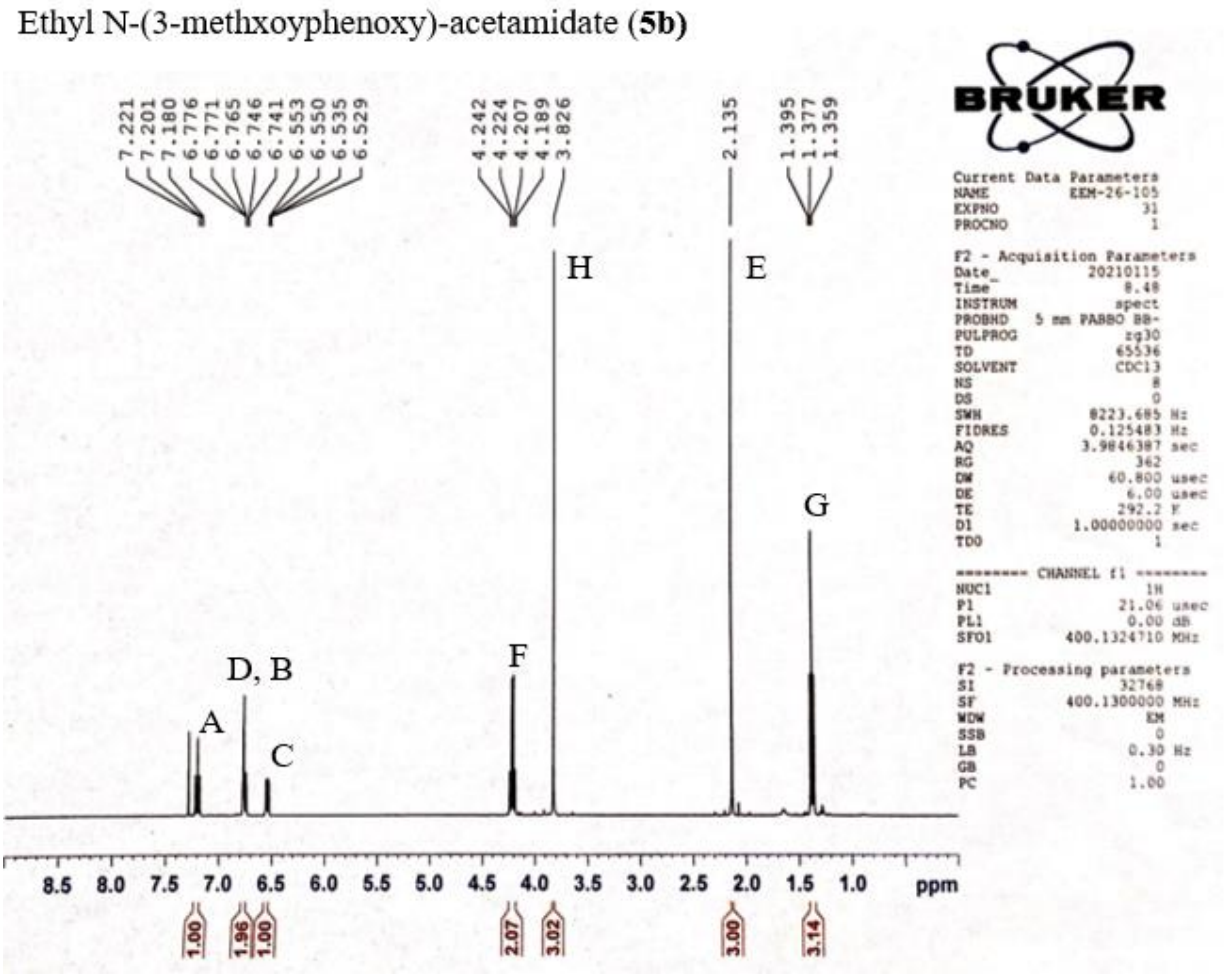

Overall, the synthesis of the ethyl N-phenoxyacetamidate derivatives (**5a-g**) was successful. After purification and verification, each derivative was used for the next reaction to prepare the O-phenylhydroxylamine derivatives (**6a-g**). The ethyl N-phenoxyacetamidate derivatives (**5a-g**) with the respective yield and percent yields are shown in Table 4.3. The derivatives, ethyl N-(4-N, N-dimethylphenoxy)-acetamidate (**5d**) and ethyl N-(4-

ethylphenoxy)-acetamidate (**5g**) were unable to produce the product through multiple tries with various heating and stirring times so the substituents were discontinued. This indicates that something else is playing a factor in the reaction for these two substituents besides being electron donating substituents. Since ethyl N-(4-methxoyphenoxy)-acetamidate (**5c**) is an electron donating substituent is able to produce the ethyl N-phenoxyacetamidate product. Each derivative was a golden-brown color and was isolated via chromatography using a hexane: ethyl acetate eluent system depending on the substituent (80:20, 90:10 or 95:5).

Table 4.3

Summary of Yields and Percent Yields of Ethyl N-phenoxyacetamidate.

Compound	Name	Time	Yield (g)	Percent yield
5a	Ethyl N-(2-methxoyphenoxy)-acetamidate	1.5	1.050	72
5b	Ethyl N-(3-methxoyphenoxy)-acetamidate	1.5	1.033	90
5c	Ethyl N-(4-methxoyphenoxy)-acetamidate	1.5	0.9236	63
5e	Ethyl N-(4-chlorophenoxy)-acetamidate	1.5	0.625	94
5f	Ethyl N-(4-fluorophenoxy)-acetamidate	2	0.796	79

The oxime hydrolysis reaction used to synthesize O-arylhydroxylamines (**6a-f)** provided moderate yields (Figure 4.5) ranging from 20% to 63%. O-Phenyllhydroxylamine hydrochloride (**6h**) was not produced in this process since it was obtained commercially.

The ethyl N-phenoxyacetamidate derivatives (**5a-f**) and 1,4-dioxane were combined and solidified. Hydrochloric acid was then added to the frozen mixture and stirred while warming from 5°C to room temperature. The warmed mixture was diluted with ether before being washed with 0.1 and 0.01 M sodium hydroxide, deionized water, and saturated brine then dried over magnesium sulfate. Full experiment details are found in Appendix A.

Figure 4.5

Synthesis for the Preparation of Substituted O-Arylhydroxylamines.

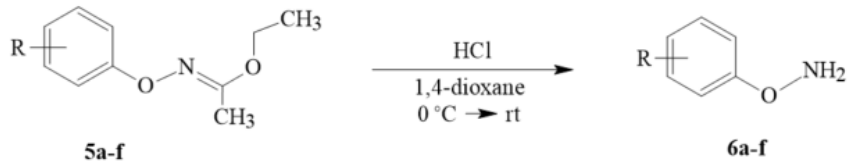

5a-f **6a-f**

The product was then gravity filtered and placed on the rotary evaporator to remove the solvent present. The dried product was diluted with dichloromethane (5-10 mL) and hydrogen chloride gas was bubbled through the product. The mixture was vacuum filtered to separate the product from the impurities. Though, the procedure should have produced the product as a solid which would be collected in the Büchner funnel of the vacuum filtration. Through multiple tries for O-arylhydroxylamine (**6a-f**), the product was found in the collected supernatant from the vacuum filtration. Both the solid particles and liquid were collected and analyzed by ^{1}H NMR spectroscopy. The product was confirmed to be in the liquid mixture. There were small traces of the product in the solid particles, however the liquid showed the product completely isolated. The yellowish-brown liquid product would turn into a dark brown solid once fully cooled to room temperature.

Table 4.4

[1]H NMR Peaks Observed for O-Arylhydroxylamine• HCl salts.

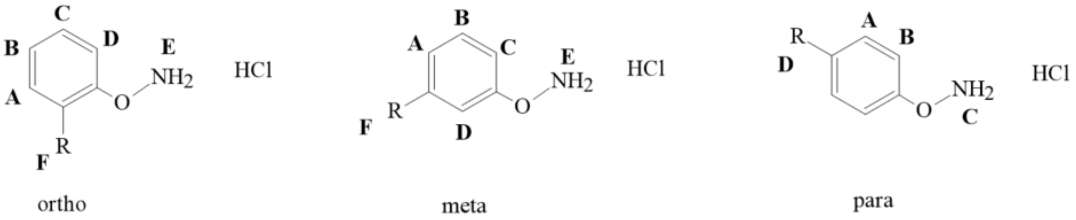

Chemical shifts of selected protons

Compound	R	A	B	C	D	E	F
6a	2-OCH_3	7.56	7.35	7.1	6.88	--	3.90
6b	3-OCH_3	7.24	7.11	6.95	7.13	--	3.78
6c	4-OCH_3	7.44	6.91	--	3.81	*	*
6e	4-Cl	7.32	7.17	--	--	*	*
6f	4-F	7.17	7.08	--	--	*	*

Note: "*" indicates that the signal would not be seen in the molecule. "--" indicates the signal was not present.

Based on Table 4.4, the amino (NH_2) signal cannot be seen in the ^1H NMR spectra (for example, see in Figure 4.6). For the substituents 4-Cl and 4-F, the NH_2 was not observed due to the NH_2 signals exchanging with the deuteroacetone solvent. The substituents 2-OCH_3 (**6a)**, 3-OCH_3 (**6b)**, and 4-OCH_3 (**6c)**, the methoxy group donates electrons into the ring, the NH_2 protons will exchange with deuterium (D), resulting in the ND_2 signal in the ^1H NMR spectrum to eliminate the expected signal. Therefore, the aromatic shifts were observed, and the lack of an ethoxy group was used to determine if the O-arylhydroxylamine product was successfully made (see Figure 4.6).

Figure 4.6

*[1]H NMR of O-(3-methoxyphenyl)hydroxylamine (**6b**).*

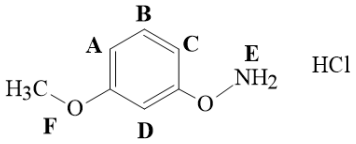

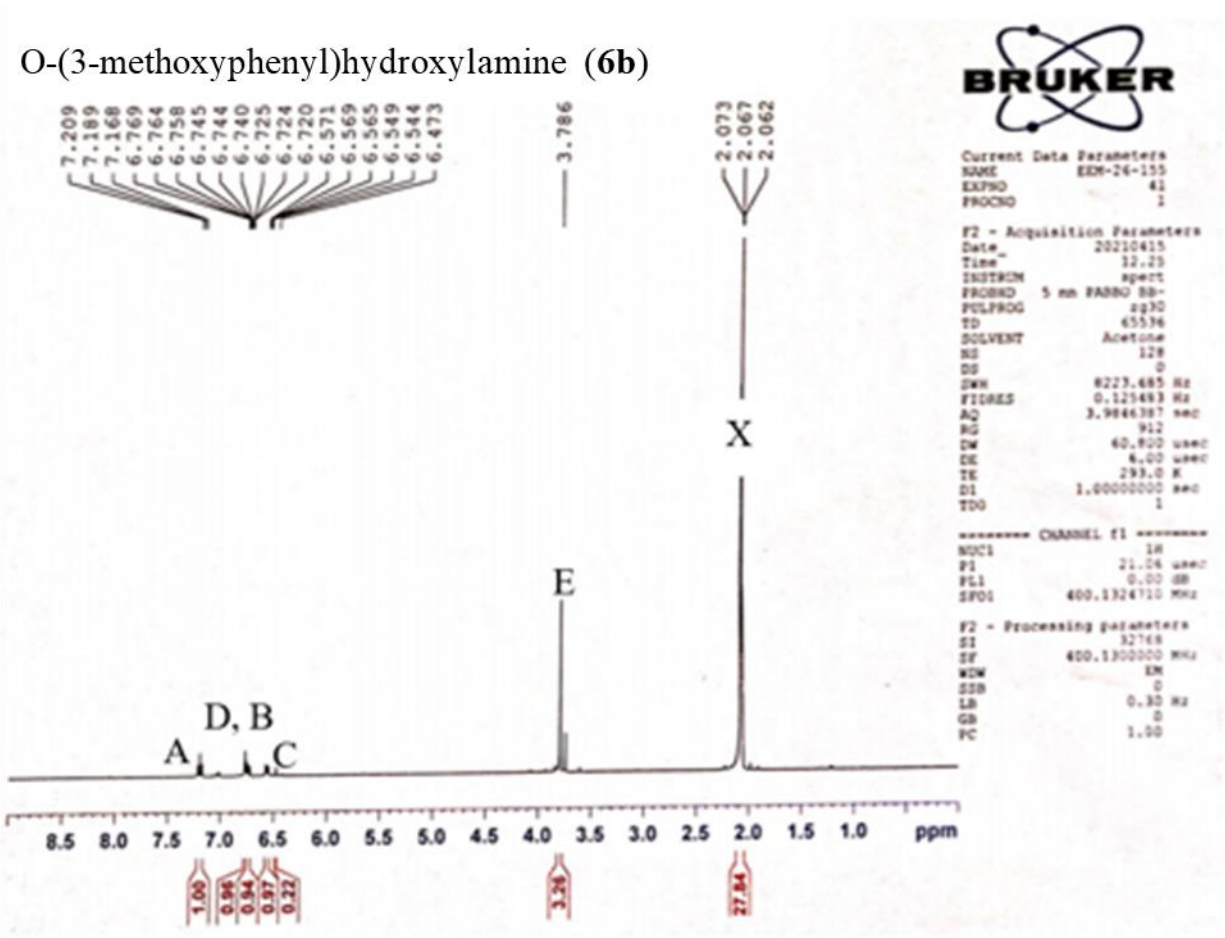

Overall, the synthesis of the O-arylhydroxylamine derivatives (**6a-f**) was successful based on the confirmation from the spectroscopic methods. After purification and verification, each derivative was used for the last reaction to prepare the O-aryl-N-(9'-acridinyl)hydroxylamine derivatives (**8a-h)**. The O-arylhydroxylamine derivatives (**6a-f**) with the respective yields and percent yields are shown in Table 4.5.

Table 4.5

Summary of Yields and Percent Yields of O-Arylhydroxylamine Derivatives.

Compound	Name	Yield (g)	Percent yield
6a	O-(2-methoxyphenyl)hydroxylamine	0.45	61
6b	O-(3-methoxyphenyl)hydroxylamine	0.46	63
6c	O-(4-methoxyphenyl)hydroxylamine	0.37	60
6e	O-(4-chlorophenyl)hydroxylamine	0.31	36
6f	O-(4-fluorophenyl)hydroxylamine	0.046	20

The last reaction in the multi-step synthesis was to prepare O-aryl-N-(9'-acridinyl)hydroxylamine derivatives (**8a-h)** by combining substituted O-arylhydroxylamine (**6a-h**) (1.5 equiv) and phenol. Once the temperature of the liquid mixture stabilized between 80-100 °C, 9-chloroacridine (**7**) (1 equiv) was added (Figure 4.7).

Figure 4.7

Synthesis for the Preparation of Substituted O-Aryl-N-(9'-acridinyl)hydroxylamines.

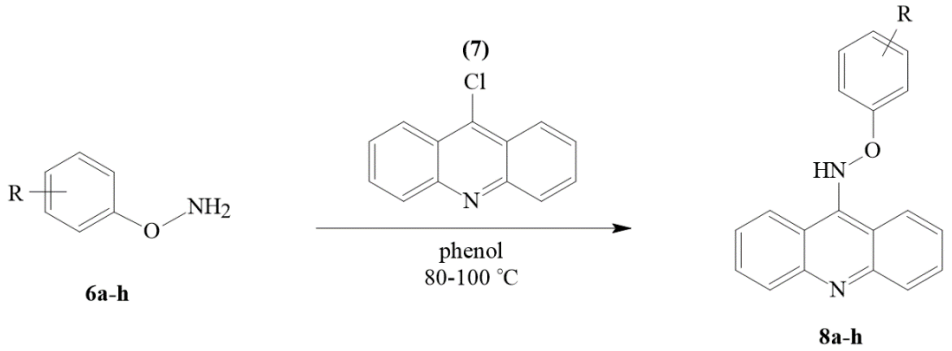

Potassium carbonate (2 mol) was added to the mixture to enhance the reactivity and cleave the salt of the hydroxylamine The reaction stirred for 12-15 hours at the stabilized temperature. Once completed, the black colored mixture was cooled to room temperature. Dichloromethane was added to dissolve the solidified mixture which revealed a dark red color.

The organic product was washed with 0.5 M NaOH, deionized water and brine to fully remove the phenol. During the extraction, the dark red color turned to a deep yellow-orange color as all the phenol was removed. The crude product was then dried over sodium sulfate and gravity filtered into a clean round bottom flask. The crude was then placed on the rotary evaporator to reduce volume to 1 mL. The crude product was then purified through a small guard column before being placed on the rotary evaporator one more time to reduce volume to 1 mL. The product was isolated through radial chromatography and confirmed through ^{1}H NMR (Figure 4.6). Each derivative collected was a brown colored compound using a particular hexane: ethyl acetate system depending on the separation (80:20, 90:10, 95:5, 98:2). Multiple separations were needed to fully isolate the O-aryl-N-(9'-acridinyl)hydroxylamine products (**8a-h**) so all or most of the hexane: ethyl acetate systems were used. Due to instrument problems, ^{1}H NMR spectra for the three O-aryl-N-(9'-acridinyl)hydroxylamines **8a**, **8e**, and **8f** were unable to be obtained which is indicated by the symbol "*" in Table 4.6.

O-aryl-N-(9'-acridinyl)hydroxylamines **8a**, **8e**, and **8f** were confirmed through thin layer chromatography by polarity and color. Retention factor (Rf) values were taken for each O-aryl-N-(9'-acridinyl)hydroxylamine (**8a-h**), as comparison using a hexane: ethyl acetate eluent system. The O-aryl-N-(9'-acridinyl)hydroxylamines (**8a-h**) are polar compounds and will present a yellow hue on the TLC plate that can be seen with the human eye. UV-light is not needed to see the isolation, but it is still used to observe the boundaries of the product and impurities during the chromatographic separation.

Table 4.6

[1]H NMR Peaks Observed for O-Aryl-N-(9'-acridinyl)hydroxylamines.

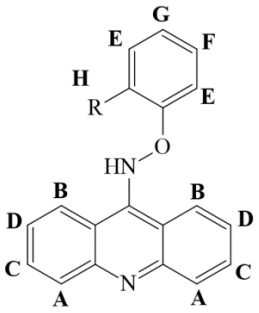

ortho

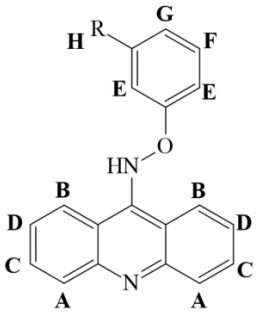

meta

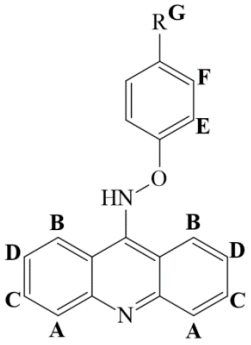

para

Chemical shifts of selected protons

Compound	R	A	B	C	D	E	F	G	H
8a	2-OCH_3	*	*	*	*	*	*	*	*
8b	3-OCH_3	8.04	7.63	7.03	6.92	5.11	5.08	4.87	3.72
8c	4-OCH_3	8.26	8.12	7.89	7.60	7.36	7.11	6.92	3.89
8e	4-Cl	*	*	*	*	*	*	*	*
8f	4-F	*	*	*	*	*	*	*	*
8h	H	8.25	8.11	7.88	7.58	7.35	7.11	6.91	--

Note: "--" indicates the signal was not present.

For the O-aryl-N-(9'-acridinyl)hydroxylamines (**8a-h**), every product presented a visible yellow hue and their Rf values can be seen in Table 4.7. The Rf values displayed values as expected with polarity of the different R groups. So, there is a high probability that products **8a**, **8e**, and **8f** are the O-aryl-N-(9'-acridinyl)hydroxylamines based on the polarity and color.

The observed yields of the O-aryl-N-(9'-acridinyl)hydroxylamines (**8a-h**) when purified were less than desired under these conditions. This is most likely due to protonation of the acridine nucleus. Based on both Forster's (2020) and Carlson's (2015) procedure, the acridine nucleus will become protonated during the chromatography significantly increasing the polarity of the compound. This increase in the presence of a non-polar mobile phase caused the

compound to tightly interact with the silica which made the separation significantly more difficult. So, triethylamine was added to the solvent system as a hindered base to decrease the polarity of the solvent system. This addition helped with the chromatographic separations however multiple separations were needed to obtain roughly complete isolation.

Table 4.7

Rf Values of O-Aryl-N-(9'-acridinyl)hydroxylamine.

Compound	Rf values
8a	0.10
8b	0.11
8c	0.12
8e	0.14
8f	0.16
8h	0.10

Note: "Rf" represents Retention factor.

O-phenyl-N-(9'-acridinyl)-hydroxylamine (**8h**) was able to be completely purified except for residual solvent (Figure 4.8) Based on Table 4.6, there was one peak exchange with the solvent used for the proton NMR which was deuteroacetone. The peak NH was not observed due to the NH signal exchanging with the deuteroacetone solvent.

Figure 4.8

*^{1}H NMR of O-Aryl-N-(9'-acridinyl)hydroxylamine (**8h**).*

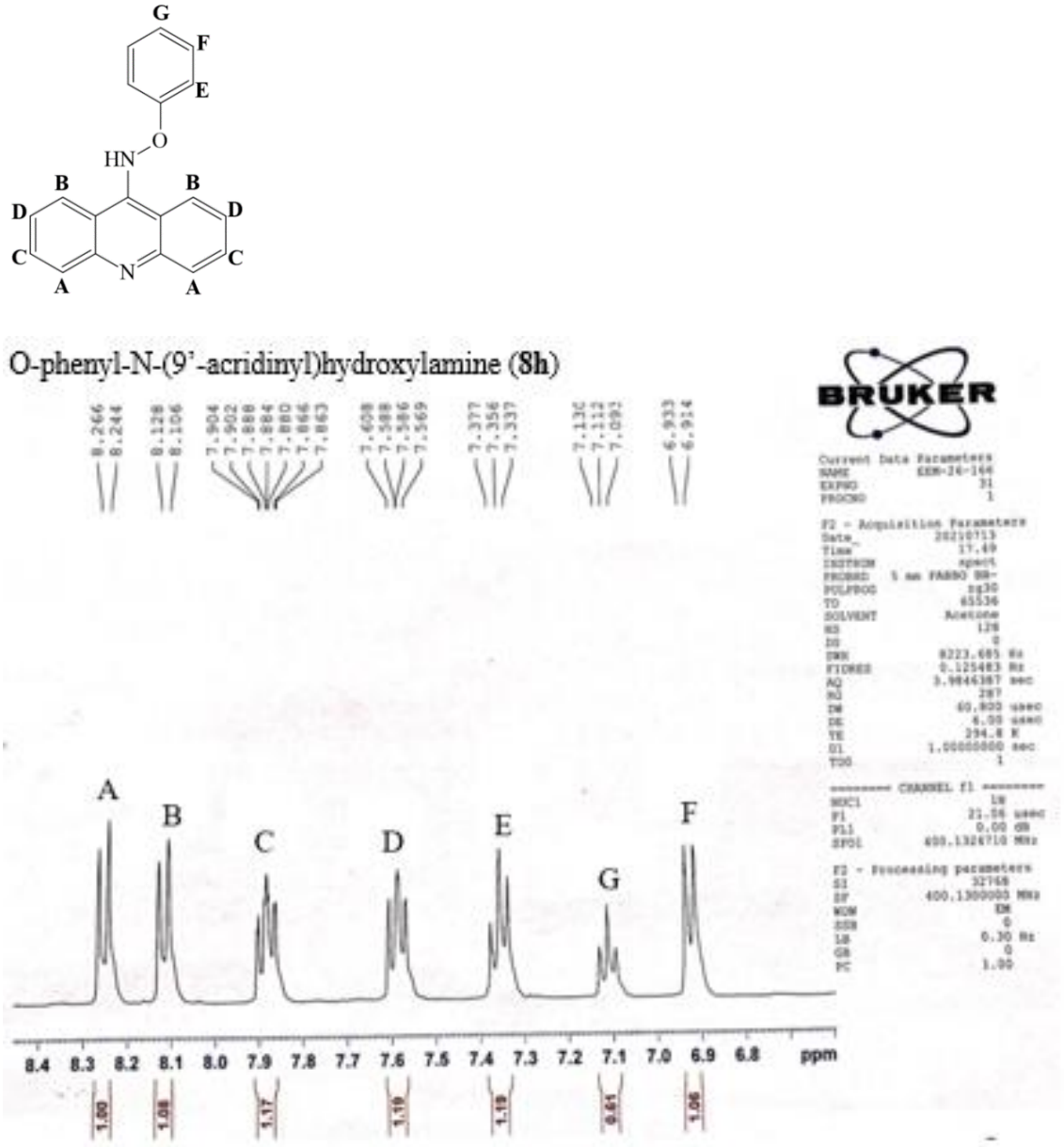

For O-(3-methoxyphenyl)-N-(9'-acridinyl)hydroxylamine (**8b**), O-(4-chloroyphenyl)-N-(9'-acridinyl)hydroxylamine (**8e**) and O-(4-fluorophenyl)-N-(9'-acridinyl)hydroxylamine (**8f**), isolation was achieved through multiple chromatographic separations. The O-(4-methoxyphenyl)-N-(9'-acridinyl)hydroxylamine (**8c**), however, was unable to be completely

purified even after multiple attempts at chromatographic separation. This is most likely due to polarity of the solvent system not being low enough to fully separate the product. Fortunately, the quantity of impurities was minimal, and the product was deemed usable for the thermal denaturation analysis with calf thymus DNA. The O-(2-methoxyphenyl)-N-(9'-acridinyl)hydroxylamine (**8a**), was also unable to be completely purified after multiple attempts at chromatographic separation. However, the quantity of impurities was minimal, and the product was deemed usable for the thermal denaturation analysis with calf thymus DNA.

The overall yield of the reactions was relatively low due to the multiple separations as described above. The product yields and percent yields are listed in Table 4.8.

Table 4.8

Summary of Yields and Percent Yields of O-Aryl-N-(9'-acridinyl)hydroxylamines.

Compound	Name	Yield (g)	Percent yield
8a	O-(2-methoxyphenyl)-N-(9'-acridinyl)hydroxylamine	0.011	15
8b	O-(3-methoxyphenyl)-N-(9'-acridinyl)hydroxylamine	0.013	17
8c	O-(4-methoxyphenyl)-N-(9'-acridinyl)hydroxylamine	0.01	16
8e	O-(4-chloroyphenyl)-N-(9'-acridinyl)hydroxylamine	0.008	6
8f	O-(4-fluorophenyl)-N-(9'-acridinyl)hydroxylamine	0.005	4
8h	O-phenyl-N-(9'-acridinyl)hydroxylamine	0.026	20

Thermal Denaturation Analysis

Each of the O-phenyl-N-(9'-acridinyl)hydroxylamines (**8a-h)** as shown in Table 4.8, were dissolved in a pH 6 phosphate buffer (0.001 M) containing 10% DMSO (10 mL) to prepare a solution that was analyzed for the compound's ability to bind to DNA. When the compound was diluted with the phosphate buffer, the solution quickly became opaque. DMSO was added as needed to make sure that the O-aryl-N-(9'-acridinyl)hydroxylamines (**8a-h**) were dissolved

without exceeding 10% volume of DMSO. Serial dilution was performed on both the DNA solution (dissolved in pH 6 phosphate buffer) and the compound solution until the concentration of both were approximately 1.0 x 10^{-6} M. The diluted solution of the appropriate O-aryl-N-(9'-acridinyl)hydroxylamines (**8a-h**) was then added to the solution of DNA to make a 1:1 molar ratio of the acridine drug to DNA. The resulting solution was kept at room temperature for an hour to reach equilibrium, then placed in a quartz cuvette in the ultraviolet-visible spectrophotometer (UV-vis). The cuvette was then slowly heated and the absorbance at 258 nm measured as a function of the temperature of the solution. Five thermal denaturation runs were completed for each O-aryl-N-(9'-acridinyl)hydroxylamine derivative to obtain an average denaturing temperature of the DNA.

To analyze each O-aryl-N-(9'-acridinyl)hydroxylamine: DNA interaction, a baseline measurement of the thermal denaturation of genomic calf-thymus DNA was conducted in a pH 6 phosphate buffer (0.001 M). The objective was to obtain the midpoint of the sigmoidal curve that would indicate where the calf thymus DNA was transitioning from double-stranded to single stranded. The thermal denaturation temperature of the calf thymus DNA was found to be 69 °C based on the data obtained from the three trials conducted. This temperature was then subtracted from each O-aryl-N-(9'-acridinyl)hydroxylamine: DNA mixture to obtain the change in thermal denaturation temperature (ΔT_m) for the specific hydroxylamine. This temperature is related to the binding constant of compound **8** with the DNA.

Each O-aryl-N-(9'-acridinyl)hydroxylamine: DNA mixture was analyzed 5 times to improve the precision of the thermal denaturation. In each case, at least one trial produced unusable data due to an improper seal on the quartz cuvette. This resulted in the evaporation of the water from the sample and an uncharacteristic increase in the absorbance of the solution that

obscured the sigmoidal curve. A standard deviation was calculated for each average thermal denaturation temperature of the specific O-aryl-N-(9'-acridinyl)hydroxylamine: DNA mixtures (Table 4.9).

Table 4.9

*Thermal Denaturation Temperatures of Each Hydroxylamine(**8a-h**): Deoxyribonucleic Acid Mixture and Average Melting Temperatures with Standard Deviation (SD).*

Compound	Trial 1	Trial 2	Trial 3	Trial 4	Trial 5	Average $T_m \pm SD$
8a	77.1	77.4	77.4	78.0	x	77.5 ± 0.4
8b	77.8	69.9	74.4	x	78.5	75.2 ± 3.9
8c	x	72.8	74.5	66.3	79.0	73.2 ± 5.3
8e	x	74.1	76.0	69.8	76.5	74.1 ± 3.1
8f	x	x	75.5	76.8	78.7	77.0 ± 1.6
8h	x	61.5	69.5	72.4	77.1	70.1 ± 6.5

Note: "x" indicates a trial with unusable data

The change in thermal denaturation temperature (ΔT_m) was obtained by taking the difference of the average denaturation temperature (T_m) of the O-aryl-N-(9'-acridinyl)hydroxylamine: DNA mixtures and the average denaturation temperature of DNA alone (Table 4.10). A tight binding of an acridine compound to DNA has a ΔT_m of 10. Based on the values in Table 4.10, the ΔT_m values of each substituted O-aryl-N-(9'-acridinyl)hydroxylamine (**8a-h**) is under 10 which indicates that there is binding to the DNA present, but the binding is most likely loose. A standard deviation was calculated for each melting temperature of the specific O-aryl-N-(9'-acridinyl)hydroxylamine: DNA mixtures (8a-h).

Table 4.10

Delta Temperatures of Each Drug: Deoxyribonucleic Acid Interaction and Average Delta Temperatures with the Deoxyribonucleic Acid Baseline.

Compound	Tm	ΔTm ± *SD*	Hammett Sigma Value, σ
8a	77.5	8.5 ± 6.0	0.08
8b	75.2	6.2 ± 4.0	0.12
8c	73.2	4.2 ± 3.0	-0.27
8e	74.1	5.1 ± 4.0	0.23
8f	77	8.0 ± 6.0	0.06
8h	70.1	1.1 ± 1.0	0

A quantitative structure activity relationship (QSAR) plot was then created for the substituted O-aryl-N-(9'-acridinyl)hydroxylamines by plotting the change in thermal denaturation temperature as the y-axis and the Hammett sigma value for each substituent that differed between the compounds as the x-axis. A linear least squares best fit line was created and the coefficient of determination, R^2, value was determined for the regression line (see Figure 4.9).

The linear least squares line indicates a potential albeit small correlation across the data. Based on the uncorrelated data and error bars, compounds that contain a substituent with a positive Hammett sigma value may have a larger change in the thermal denaturation temperature. This indicates that electron withdrawing groups improve the interaction between DNA and the O-aryl-N-acridinyl-hydroxylamine. The withdrawal of electron density from the acridine (by the aryl substituent) is predicted to make the acridine more likely to accept pi-stacking interactions from the DNA base pairs, which may be the reason for the slight increase in thermal denaturation temperatures.

Figure 4.9

*Correlation Plot for Prepared Series of Substituted O-Aryl-N-(9'-acridinyl)hydroxylamines (**8a-h**) Relating ΔT_m and Hammett Sigma Values.*

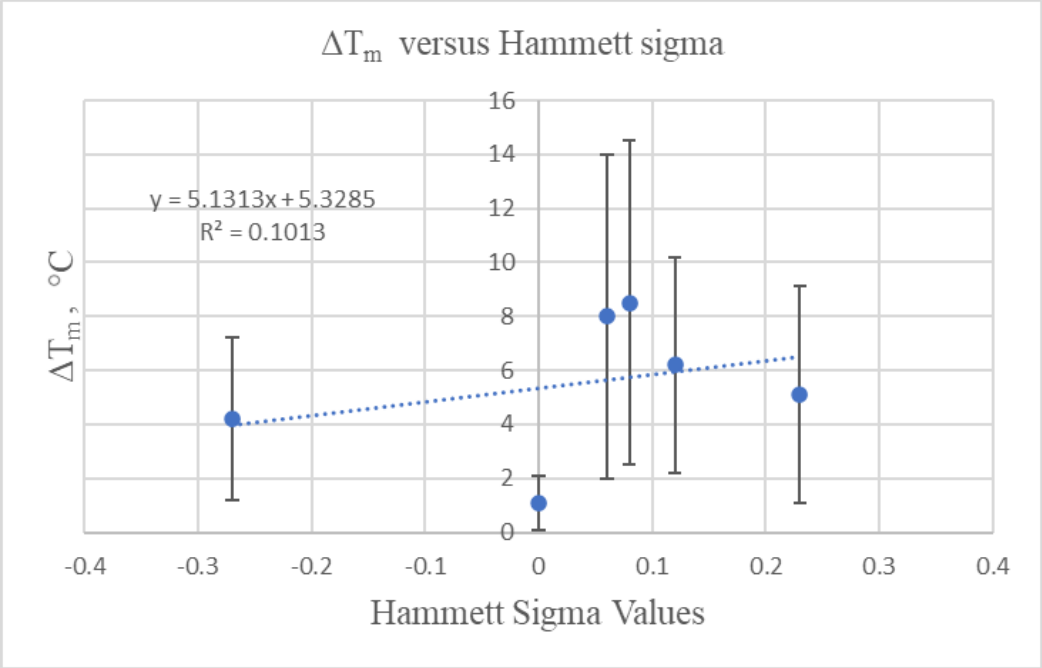

The change in thermal denaturation temperatures for each of the compounds in this study is fairly small. A typical acridine-like single intercalative event is expected to have a ΔT_m of 10°C. Thus, the compounds examined in this study have less than the equivalent of one intercalative event per molecule. This does not imply that these compounds are ineffective in causing cell apoptosis as there are additional interactions *in vivo* that are not indicated by a thermal denaturation temperature measurement.

Unfortunately, due to an issue with the department NMR, spectra of **8a**, **8b**, **8c**, **8e**, and **8f** were unable to be obtained before completing the thermal denaturation analysis. Instead, thin-layer chromatography was used to determine the identity of the compound and its purity before the analysis. The NMR spectra do reveal that there may be some impurities in the isolated products. These impurities could cause issues to arise during the thermal denaturation analysis.

In other words, the small changes in the thermal denaturation temperatures observed in each of the compound **8** solutions could be the result of the effective ‘dilution’ of the pure compound with impurities or due to the presence of the impurities themselves.

As indicated, compound **8h** gave the most precise results from the thermal denaturation analysis. Compound **8h** was completely isolated and its identity and purity confirmed through both thin-layer chromatography and NMR before the NMR instrument problems occurred. The precursor to **8h**, O-arylhydroxylamine• HCl salt **6h**, was commercially obtained and may have had an influence in the O-aryl-N-(9’-acridinyl)hydroxylamines (**8h)** product being produced since it was completely pure.

CHAPTER V

CONCLUSIONS

The reaction sequence developed to prepare compounds **8a-h** involved three steps. The first step, a palladium coupling reaction, provided the expected ethyl N-phenoxyacetamidates. The formation of the product was easily monitored, although the reaction yield was relatively low. In the second step of the sequence, hydrochloric acid and dioxanes were used to produce the expected O-arylhydroxylamine• HCl salt product. A modification, involving the isolation of the product as the hydrochloride salt resulted in an increased yield. This allowed the production of quantities of the hydroxylamine that were crucial in the final step of the synthetic sequence.

In that final step, a series of substituted O-aryl-N-(9'-acridinyl)hydroxylamines (**8a-h**) were synthesized and identified by spectroscopic methods. Each derivative was evaluated for purity using thin-layer chromatography. The purification step in the synthesis of each derivative proved challenging; however, after exploration of the methods, a 3-step chromatographic separation using radial chromatography was developed that provided **8a-h** as a single compound. Unfortunately, thin-layer chromatography was the best determinant of purity because of issues with the department NMR after the first compound (**8h**) was made and purified.

The results shown in Figure 4.8 proved that the O-aryl-N-(9'-acridinyl)hydroxylamine could be fully isolated after numerous chromatographic separations. Compounds **8a**, **8b**, **8c**, **8e**, and **8f** unfortunately were not able to be fully isolated but the impurities were minimal as determined by thin-layer chromatography and the sparse information from the NMR.

A solution containing compound **8** was made in a phosphate buffer and used to determine the ability of the compound to bind to DNA. A phosphate buffered solution of genomic calf thymus DNA was evaluated for the temperature at which it transitioned from double-stranded to single-stranded. Then, the DNA solution was combined with each of the compound **8** solutions, incubated to allow the hydroxylamine to interact with the DNA, and the thermal denaturation temperature measured.

A thermal denaturation profile was collected for each substituted O-aryl-N-(9'-acridinyl)hydroxylamine and compared with the thermal denaturation profile of calf thymus DNA. Each thermal denaturation profile differed in its appearance by a higher temperature transition than genomic calf-thymus DNA alone. The differences were reduced to the effect of each specific substituent on compound **8**. A quantitative structure activity relationship (QSAR) was developed based on the differences in the electronic character of those substituents. The specific physiochemical parameter used for the correlation was the Hammett sigma value. A plot of the Hammett sigma (x-axis) with the change in the thermal denaturation of calf-thymus DNA (y-axis) was then prepared.

No linear correlation could be constructed from that data. On the plot, the greatest impact to the thermal denaturation temperature was observed with substituents that had a positive Hammett sigma value. This indicated that electron donating substituents had a greater impact than electron withdrawing substituents on the thermal denaturation temperature.

Based on Table 4.10, the change in thermal denaturation temperature for each substituted O-aryl-N-(9'-acridinyl)hydroxylamine **8a-h**, was small. Typically, acridine compounds will have a ΔT_m of 10°C in a single intercalative event. Based on the data presented in Table 4.10 and the impurities presence in the **8a**, **8b**, **8c**, **8e** and **8f** products, the standard deviation is not very good.

This indicates that the correlation between the O-aryl-N-(9'-acridinyl)hydroxylamine products and the calf-thymus DNA is likely very weak and not very good. However, this does not suggest that the O-aryl-N-(9'-acridinyl)hydroxylamines (**8a-h**) are ineffective in generating cell apoptosis. Thermal denaturation temperature measurements only indicate one interaction between the O-aryl-N-(9'-acridinyl)hydroxylamine products and calf thymus DNA. There are multiple interactions that have yet to be explored that are not indicated by thermal denaturation.

With the weak correlation observed between the O-aryl-N-(9'-acridinyl)hydroxylamines and the calf thymus DNA (Figure 4.9) there is a possibility that there is no correlation with the electronic effects of the different substituents presented in the series. As seen in Table 4.10, the substituents have different Hammett sigma values ranging from -0.27 to 0.23. This range of Hammett sigma values suggests that there should be a variety of electronic effects based on the different magnitudes of σ values. This, however, was not completely supported by the data presented in the thermal denaturation analysis (see Figure 4.9 and Table 4.10).

Despite the thermal denaturation analysis data not fully supporting the original claim of there being a correlation with the various electronic effects, there could still be a correlation between the electronic effects. Errors must be taken into consideration on why the data might have not support the original claim. One possible error that could be the result of the small correlation present in the QSAR plot is the quantity of impurities present in the different O-aryl-N-(9'-acridinyl)hydroxylamines (**8a-f**). The impurities could have had an impacted on the thermal denaturation analysis and muted the O-aryl-N-(9'-acridinyl)hydroxylamine's effect on the DNA, but further investigation is needed to confirm.

The other possible error that could have resulted the small correlation is the oxime hydrolysis step. In the hydrolysis step, acetone-d_6 was used to confirm the product in the NMR. It

is possible that residual acetone in the acetone-d_6 presented the amino signal in the spectra instead of the O-arylhydroxylamine• HCl salt product. The amine signal did have a molar ratio consistent with the O-arylhydroxylamine• HCl salt product, however there is still a small possibly the signal was not from the salt product. Further investigation is needed to confirm if the oxime hydrolysis step cleaves off the oxime specifically or more than originally thought and supported by the mechanism in Figure 3.6. Deuterated chloroform ($CDCl_3$-d) should be used during the future investigation to confirm in the amino signal is in fact from the O-arylhydroxylamine• HCl salt product or not.

In the future, development of other methods to fully isolate the library of O-aryl-N-(9'acridinyl)hydroxylamines compounds should be studied to improve their purity and yield. Other substituents should be studied though the method described above or through a new method. The purity of the O-aryl-N-(9'-acridinyl)hydroxylamine product should be confirmed through full spectroscopic characterization. The hydrolysis of the ethyl N-phenoxyacetamidates to the O-arylhydroxylamine• HCl salt product should be measured to see if the hydroxylamine increases the half-life of the compound. The O-arylhydroxylamine• HCl salt product should be tested through the NMR instrument with a different solvent other than acetone-d_6 to confirm the amino functional group as well. Furthermore, another evaluation should be performed, such as DNA viscosity or *in vivo* measurements of apoptosis should be explored for a library of O-aryl-N-(9'acridinyl)hydroxylamines to evaluate and determine the effect of the substituents' impact on the binding ability and transition temperature of double-stranded DNA to single-stranded DNA.

REFERENCES

Abis, L., Sen, A., & Halpern, J. (1978). Intramolecular reductive elimination of alkanes from cis-hydridoalkylbis (phosphine) platinum (II) complexes. *Journal of the American Chemical Society*, *100*(9), 2915-2916.

Ageno, M., Dore, E., & Frontali, C. (1969). The alkaline denaturation of DNA. *Biophysical Journal*, *9*(11), 1281–1311.

Aykul, S., & Martinez-Hackert, E. (2016). Determination of half-maximal inhibitory concentration using biosensor-based protein interaction analysis. *Analytical Biochemistry*, *508*, 97-103.

Blake, R. D., & Delcourt, S. G. (1996). Thermodynamic effects of formamide on DNA stability. *Nucleic acids research*, *24*(11), 2095-2103.

Bragato, M., von Rudorff, G. F., & von Lilienfeld, O. A. (2020). Data enhanced Hammett-equation: reaction barriers in chemical space. *Chemical science*, *11*(43), 11859-11868.

Carlson, A. L. (2015). *O-benzyl-N-(9'-acridinyl)-hydroxylamines as Potential Antitumor Agents* (Doctoral dissertation, University of Northern Colorado).

Charmantray, F., & Martelli, A. (2001). Interest of acridine derivatives in the anticancer chemotherapy. *Current pharmaceutical design*, *7*(17), 1703-1724.

Chavalitshewinkoon, P. O. R. N. T. I. P., Wilairat, P., Gamage, S., Denny, W., Figgitt, D., & Ralph, R. (1993). Structure-activity relationships and modes of action of 9-anilinoacridines against chloroquine-resistant Plasmodium falciparum in vitro. *Antimicrobial agents and chemotherapy*, *37*(3), 403-406.

Denny, W. A. (2002). Acridine derivatives as chemotherapeutic agents. *Current Medicinal Chemistry*, *9*(18), 1655-1665.

Denny, W. A., Atwell, G. J., & Baguley, B. C. (1983). Potential antitumor agents. Part 38. 3-Substituted 5-carboxamido derivatives of amsacrine. *Journal of medicinal chemistry*, *26*(11), 1619-1625.

Forster, J. (2020). Synthesis and Evaluation of N-(9'-Acridinyl)-O-phenylhydroxylamines.

Georghiou, S. (1977). Interaction of acridine drugs with DNA and nucleotides. *Photochemistry and photobiology*, *26*(1), 59-68.

Hansch, C., Kurup, A., Garg, R., & Gao, H. (2001). Chem-bioinformatics and QSAR: a review of QSAR lacking positive hydrophobic terms. *Chemical Reviews*, *101*(3), 619-672.

Hammett, L. P. (1937). The effect of structure upon the reactions of organic compounds. Benzene derivatives. *Journal of the American Chemical Society*, *59*(1), 96-103.

Jang, Y., Son, H., Lee, S. W., Hwang, W., Jung, S. R., Byl, J. A. W., Osheroff, N., & Lee, S. (2019). Selection of DNA cleavage sites by topoisomerase II results from enzyme-induced flexibility of DNA. *Cell chemical biology*, *26*(4), 502-511.

Johnson, C. D. (1973). *The Hammett equation.* University Press.

Maimone, T. J., & Buchwald, S. L. (2010). Pd-catalyzed O-arylation of ethyl acetohydroximate: synthesis of O-arylhydroxylamines and substituted benzofurans. *Journal of the American Chemical Society*, *132*(29), 9990-9991.

Mayo Clinic. (2021). *Cancer*. https://www.mayoclinic.org/diseases-conditions/cancer/symptoms-causes/syc-20370588?p=1

McClendon, A. K., Rodriguez, A. C., & Osheroff, N. (2005). Human topoisomerase IIα rapidly relaxes positively supercoiled DNA: implications for enzyme action ahead of replication forks. *Journal of Biological Chemistry*, *280*(47), 39337-39345.

Nelson, D. L., Lehninger, A. L., & Cox, M. M. (2008). *Lehninger principles of biochemistry*. Macmillan.

Rowe, T. C., Chen, G. L., Hsiang, Y. H., & Liu, L. F. (1986). DNA damage by antitumor acridines mediated by mammalian DNA topoisomerase II. *Cancer Research*, *46*(4 Part 2), 2021-2026.

Russell, A. P., & Holleman, D. S. (1974). The thermal denaturation of DNA: average length and composition of denatured areas. *Nucleic Acids Research*, *1*(8), 959-978.

Sirajuddin, M., Ali, S., & Badshah, A. (2013). Drug–DNA interactions and their study by UV–Visible, fluorescence spectroscopies and cyclic voltametry. *Journal of Photochemistry and Photobiology B: Biology*, *124*, 1-19.

Wadkins, R. M., & Graves, D. E. (1989). Thermodynamics of the interactions of m-AMSA and o-AMSA with nucleic acids: influence of ionic strength and DNA base composition. *Nucleic acids research*, *17*(23), 9933-9946.

Wang, X., Lim, H. J., & Son, A. (2014). Characterization of denaturation and renaturation of DNA for DNA hybridization. *Environmental health and toxicology*, *29*.

Wilson, W. R., Baguley, B. C., Wakelin, L. P., & Waring, M. J. (1981). Interaction of the antitumor drug 4'-(9-acridinylamino) methanesulfon-m-anisidide and related acridines with nucleic acids. *Molecular Pharmacology*, *20*(2), 404-414.

World Health Organization. (2021). *Cancer*. https://www.who.int/news-room/fact-sheets/detail/cancer.

Valdés, A. F. C. (2011). Acridine and acridinones: old and new structures with antimalarial activity. *The Open Medicinal Chemistry Journal*, *5*, 11.

APPENDIX A

EXPERIMENTAL DATA

Preparation of Substituted Ethyl N-phenoxyacetamidates (5a-f).

An oven-dried 50 mL round bottom flask cooled with argon to room temperature. Once cooled, 490 mg of cesium carbonate (1.5 mmol, 1.5 equiv) was added followed by 7 mg of allylpalldium (II) dichloride (**3**, 2 mol%), 21 mg of t-butylbrettphos (**4**, 4 mol %), and the aryl bromide (if solid): **1c** (1.0 mmol, 1.0 equiv). The round bottom flask was continuously filled with argon and capped. To the sealed flask, the aryl bromide was added (if liquid): **1a, 1b, 1c, 1d, 1f, 1g** followed by 2.0 mL of anhydrous toluene, and 0.12 mL of ethyl acetohydroxamate (**2**, 1.25 mmol, 1.25 equiv.). With a continuous flow of argon, the round bottom flask was transferred into a preheated 65-70 °C oil bath and stirred for 1-4 hours (see Table 4.3). The round bottom flask was removed from the oil bath and cooled to room temperature and a TLC evaluation of the reaction mixture was obtained. Radial chromatography was used to separate the product mixtures. The products **5a-f** were used in the subsequent steps without additional purification.

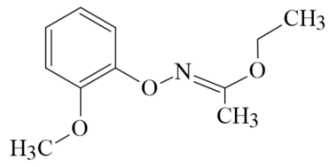

Ethyl N-(2-methxoyphenoxy)-acetimidate, 5a

Yield: 72% (1.050 g). ^{1}H NMR (400 MHz, $CDCl_3$-d) δ 7.56 (m, 2H), 7.31 (d, J= 7.2 Hz, 2H), 6.93 (d, J= 8 Hz, 2H), 6.86 (t, J= 7.6 Hz, 2H), 4.14 (q, J= 7.2 Hz, 2H), 3.92 (s, 3H), 2.07 (s, 3H), 1.28 (t, J= 7.2 Hz, 3H) ppm.

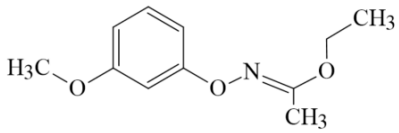

Ethyl N-(3-methxoyphenoxy)-acetimidate, 5b

Yield: 90% (1.033 g). ^{1}H NMR (400 MHz, $CDCl_3$-d) δ 7.22 (t, J= 8 Hz, 2H), 6.77 (d, J= 2.2 Hz, 2H), 6.74 (d, J= 2.0 Hz, 2H), 4.24 (q, J= 7.2 Hz, 2H), 3.82 (s, 3H), 2.13 (s, 3H), 1.37 (t, J= 7.2 Hz, 3H) ppm.

Ethyl N-(3-methoxyphenoxy)-acetimidate, (**5b**)

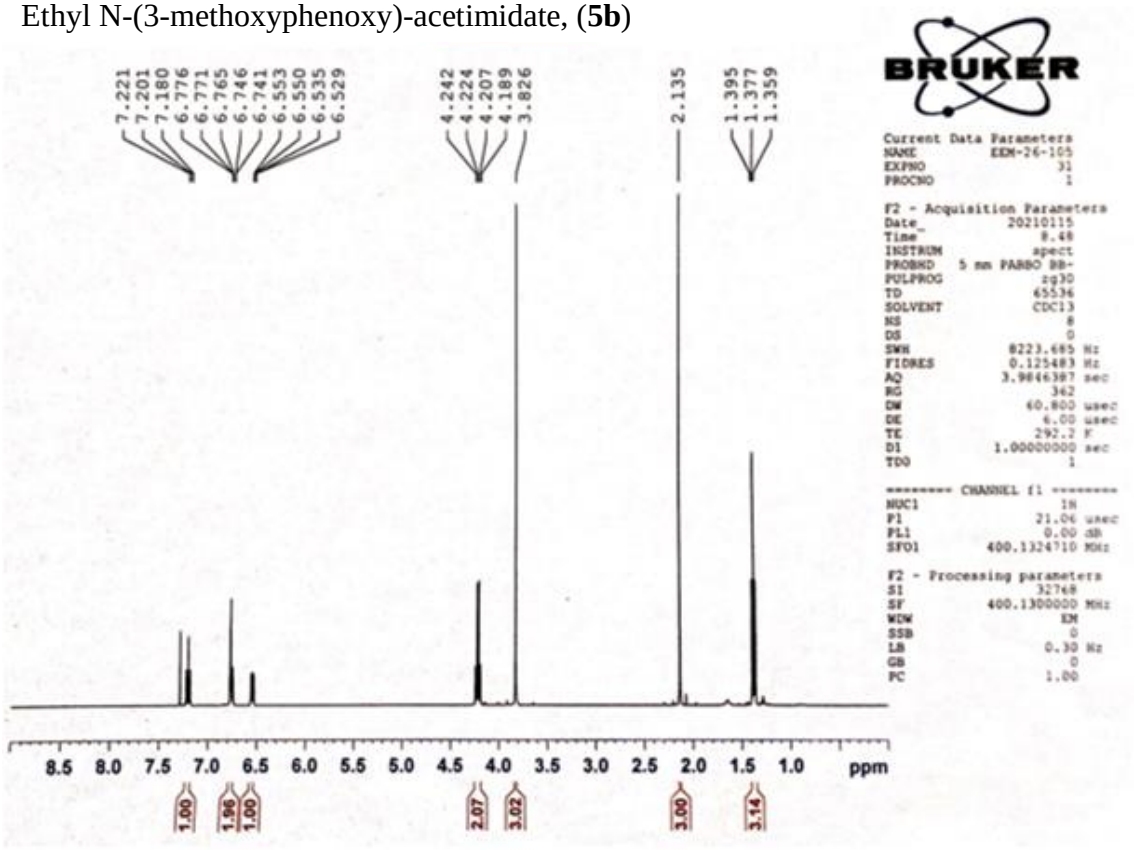

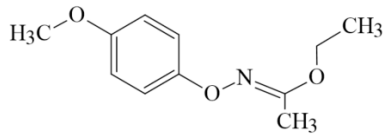

Ethyl N-(4-methxoyphenoxy)-acetimidate, 5c

Yield: 63% (0.9236 g). ^{1}H NMR (400 MHz, $CDCl_3$-d) δ 7.09 (d, J= 9.2 Hz, 2H), 6.85 (d, J= 8.8 Hz, 2H), 4.19 (q, J= 7.2 Hz, 2H), 3.80 (s, 3H) 2.10 (s, 3H), 1.36 (t, J= 6.8 Hz, 3H) ppm.

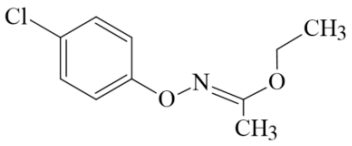

Ethyl N-(4-chlorophenoxy)-acetimidate, 5e

Yield: 94% (0.625 g). ^{1}H NMR (400 MHz, $CDCl_3$-d) δ 7.26 (m, 2H), 7.10 (d, J= 9.6 Hz, 2H), 4.2 (q, J= 7.2 Hz, 2H), 2.13 (s, 3H), 1.37 (t, J= 6.8 Hz, 3H) ppm.

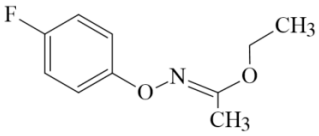

Ethyl N-(4-fluorophenoxy)-acetimidate, 5f

Yield: 79% (0.796 g). ^{1}H NMR (400 MHz, $CDCl_3$-d) δ 7.09 (m, 2H), 6.98 (t, J= 8.4 2H), 4.20 (q, J= 7.2 Hz, 2H), 2.13 (s, 3H), 1.37 (t, J= 6.8 Hz, 3H) ppm.

General procedure for the preparation of substituted O-arylhydroxylamines (6a-f).

To a 50-100 mL round bottom flask, 0.75 mmol (1 equiv) of the substituted ethyl-N-phenoxyacetamidate (**5a-f**) and 1.5 ml of 1,4-dioxane was combined. The round bottom flask was capped and placed in the freezer until the mixture solidified. Once the mixture solidified, the round bottom flask was removed from the freezer and placed into an ice bath. Approximately, 4.5 mmol of concentrated hydrochloric acid was added (6 M aqueous solution, 750 µl, 6 equiv) and the mixture stirred for 6 minutes. With the mixture becoming a liquid again, the liquid was taken out of the ice bath and left to stir for 1-2 at room temperature. After stirring, the mixture was diluted with diethyl ether and transferred to a separatory funnel. Approximately, 25 mL of 0.1 M NaOH was added to the mixture before the aqueous layer was extracted. The organic layer was washed with 0.1 M NaOH (25 mL) until the aqueous layer had a basic pH. The organic layer was then washed with 0.01 M NaOH, deionized water and saturated brine separately before being dried over magnesium sulfate ($MgSO_4$). The organic phase was then gravity filtered into a clean round bottom flask evaporated to dryness using a rotary evaporator. The crude product mixture was then dissolved in dichloromethane (5-10 mL) and hydrogen chloride gas was bubbled through the resulting solution. The product was still in a liquid phase, so it was vacuum filtered then placed on the rotary evaporator to remove the solvent. The product would later turn solid once fully cooled to room temperature. The yields were calculated, and the products **6a-f** was verified using ^{1}H NMR spectroscopy.

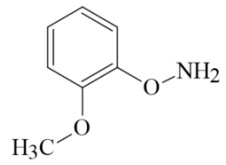

O-(2-methoxyphenyl)hydroxylamine, 6a

Yield 61% (0.45 g). ^{1}H NMR (400 MHz, acetone-d_6) in δ 7.56 (m, 1H) 7.31 (m, 1H), 7.10 (d, J= 8 Hz, 2H), 6.88 (m, 2H), 3.90 (s, 3H) ppm.

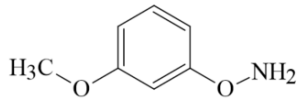

O-(3-methoxyphenyl)hydroxylamine, 6b

Yield 63% (0.46 g). ^{1}H NMR (400 MHz, acetone-d_6) in δ 7.24 (t, J= 8 Hz, 2H), 7.13 (m, 2H), 6.95 (m, 2H), 3.78 (s, 3H) ppm. The solvent peak is indicated by the "X" on the spectra.

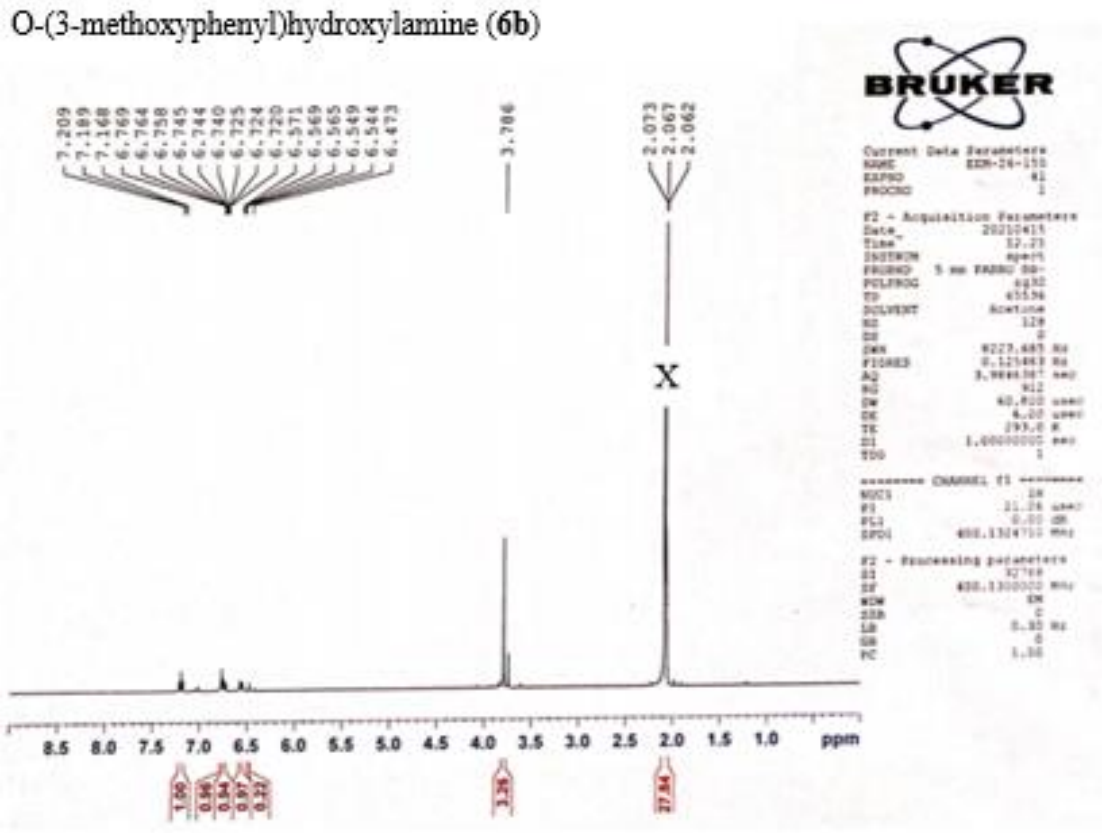

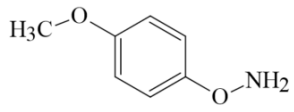

O-(4-methoxyphenyl)hydroxylamine, 6c

Yield 60 % (0.37 g). ^{1}H NMR (400 MHz, acetone-d_6) in δ 7.44 (d, J= 8.8 Hz, 2H), 6.91 (d, J= 8.8 Hz, 2H), 3.81 (s, 3H) ppm.

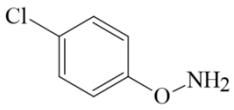

O-(4-chlorophenyl)hydroxylamine, 6e

Yield 36% (0.31 g). ^{1}H NMR (400 MHz, acetone-d_6) in δ 7.32 (d, J= 8.8 Hz, 2H), 7.17 (m, 2H), 6.85 (d, J= 8.8 Hz, 2H) ppm.

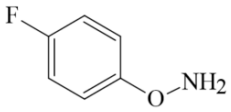

O-(4-fluorophenyl)hydroxylamine, 6f

Yield 20% (0.046 g). ^{1}H NMR (400 MHz, acetone-d_6) in δ 7.17 (d, J= 6.4 Hz, 2H) 7.08 (d, J=9.2 Hz, 2H), 3.31 (s, 3H) ppm.

General procedure for preparation of O-aryl-N-(9'-acridinyl)hydroxylamines (8a-h)

The appropriate **s**ubstituted O-arylhydroxylamine (**8a-h,** 1.5 mol) and potassium carbonate (2 mol) (if hydroxylamine was a salt) was treated with 9-chloroacridine (**7**) (1 mol). The reaction was performed in molten phenol using 3.0 grams of phenol per gram of 9-chloroacridine (**7**). The reaction was heated between 80-100 °C for 12-15 hours. The reaction mixture was cooled to room temperature after stirring and dissolved in dichloromethane. The organic product was washed with 0.5 M NaOH (25 mL x 3), deionized water (25mL), and saturated brine (25mL). The organic layer was dried over anhydrous sodium sulfate and gravity filtered to a clean RB. The crude product was evaporated to a volume of approximately of 1 mL then passed through a short guard column wetted with ethyl acetate. The crude product was again dried to a volume of approximately 1 mL before being separated using radial chromatography. A 1- or 2-mm circular plate (silica gel, 2mm) was placed in the chromatotron and wetted with a hexanes and ethyl acetate mixture containing 5% triethylamine system. The amount of the crude would indicate which circular plate would be used. A 1 mm plate will hold 0.100 grams or less of crude product and a 2 mm plate will hold between 0.100 to 0.200 grams of crude product. Once the plate was wetted, the crude product was injected onto the plate and the separation of the individual components guided using a UV lamp. The product was collected over several fractions. The similar fractions were combined, and the solvent was removed using rotary evaporation. For each crude product, two to five separations were preformed to fully isolate the product. A ^{1}H NMR was collected for each of the collected bands to verify product and the yields of the desired product were determined.

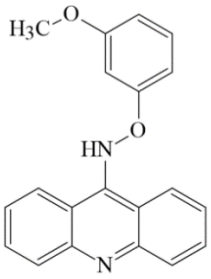

O-(2-methoxyphenyl)-N-(9'-acridinyl)hydroxylamine, 8a

Compound 8a was isolated as a yellow solid. TLC Rf (0.10), yellow hue.

Yield: 15% (0.011 g). ^{1}H NMR (400 MHz, acetone-d_6) showed presence of compound; however, mixture was impure. “Rf” represents Retention factor.

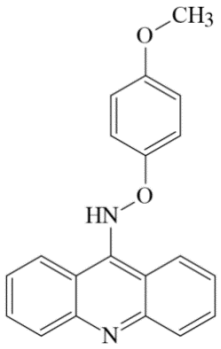

O-(3-methoxyphenyl)-N-(9'-acridinyl)hydroxylamine, 8b

Compound 8a was isolated as a brown solid. TLC Rf (0.11), yellow hue. Yield: 17% (0.013 g). ^{1}H NMR (400 MHz, acetone-d_6) showed presence of compound; however mixture was impure. “Rf” represents Retention factor.

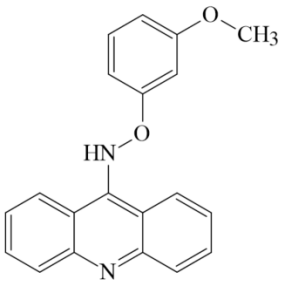

O-(4-methoxyphenyl)-N-(9'-acridinyl)hydroxylamine, 8c

Compound 8c was isolated as a yellow solid. TLC Rf (0.12), yellow hue. Yield: 16% (0.01 g). ^{1}H NMR (400 MHz, acetone-d_6) showed presence of compound; however, mixture was impure. "Rf" represents Retention factor.

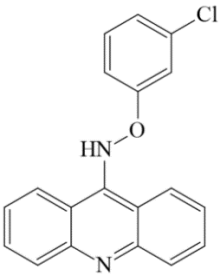

O-(4-chloroyphenyl)-N-(9'-acridinyl)hydroxylamine, 8e

Compound 8e was isolated as an orange solid. TLC Rf (0.14), yellow hue. Yield 6% (0.008 g). ^{1}H NMR (400 MHz, acetone-d_6) showed presence of compound; however, mixture was impure. "Rf" represents Retention factor.

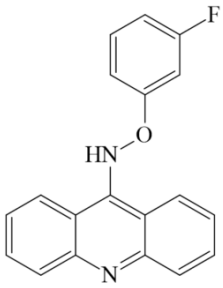

O-(4-fluoroyphenyl)-N-(9'-acridinyl)hydroxylamine, 8f

Compound 8f was isolated as an orange solid. TLC Rf (0.16), yellow hue. Yield 4% (0.005 g).

^{1}H NMR (400 MHz, acetone-d_6) showed presence of compound; however, mixture was impure.

“Rf” represents Retention factor.

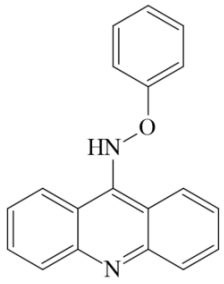

O-phenyl-N-(9'-acridinyl)hydroxylamine, 8h

Compound 8h was isolated as a brown solid. TLC Rf (0.1), yellow hue. Yield: 20% (0.026 g). ^{1}H NMR (400 MHz, acetone-d_6) in δ: 8.25 (d, J= 8.8 Hz, 1H), 8.11 (d, J= 8.8 Hz, 1H), 7.88 (m, 1H), 7.59 (m, 1H), 7.35 (t, J= 8 Hz, 3H), 7.11 (t, J= 7.2 Hz, 2H), 6.91 (d, J= 7.6 Hz, 2H) ppm. 13CNMR data (acetone-d6) δ: -748509.5; -748511.0; -748512.0; -748516.8; -748517.0; -748517.2; -748518.2; -748518.9; -748519.1; -748519.6; -748520.8 ppm. The solvent peak is indicated by the "X" on the spectra. "Rf" represents Retention factor.

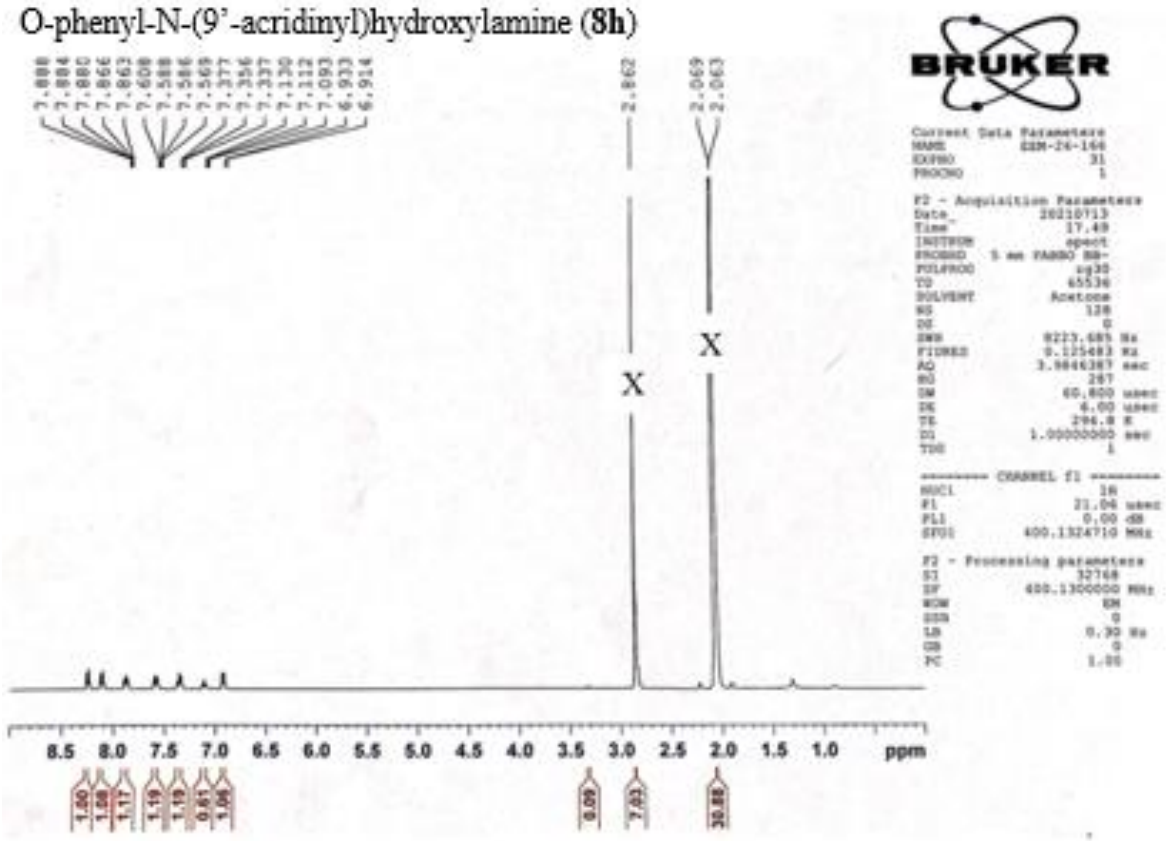

O-phenyl-N-(9'-acridinyl)hydroxylamine (**8h**)

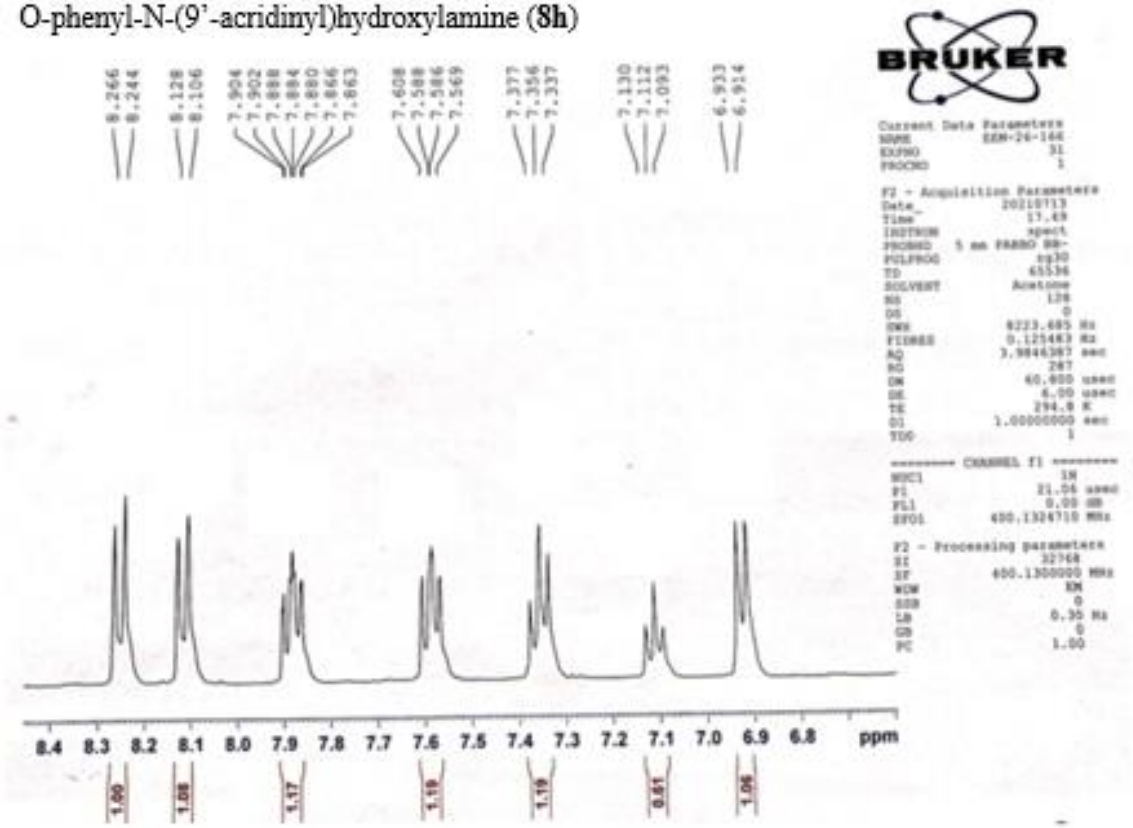

O-phenyl-N-(9'-acridinyl)hydroxylamine (**8h**)

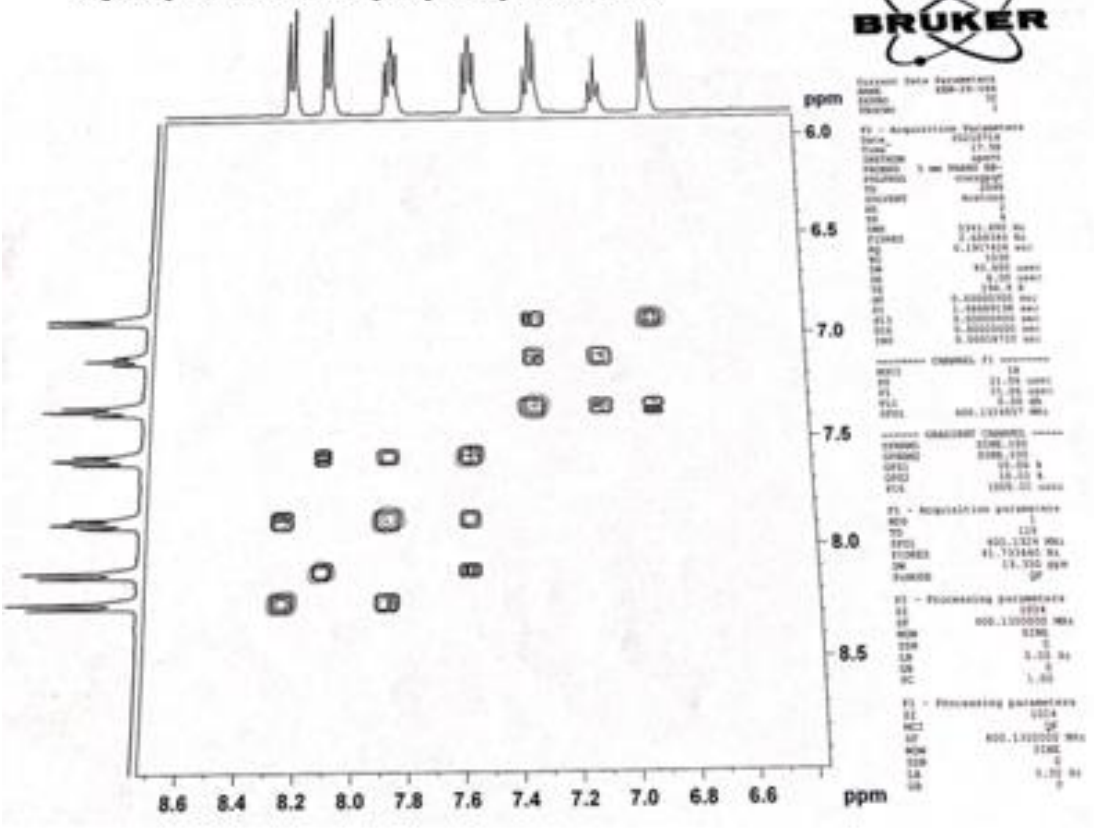

O-phenyl-N-(9'-acridinyl)hydroxylamine (**8h**)

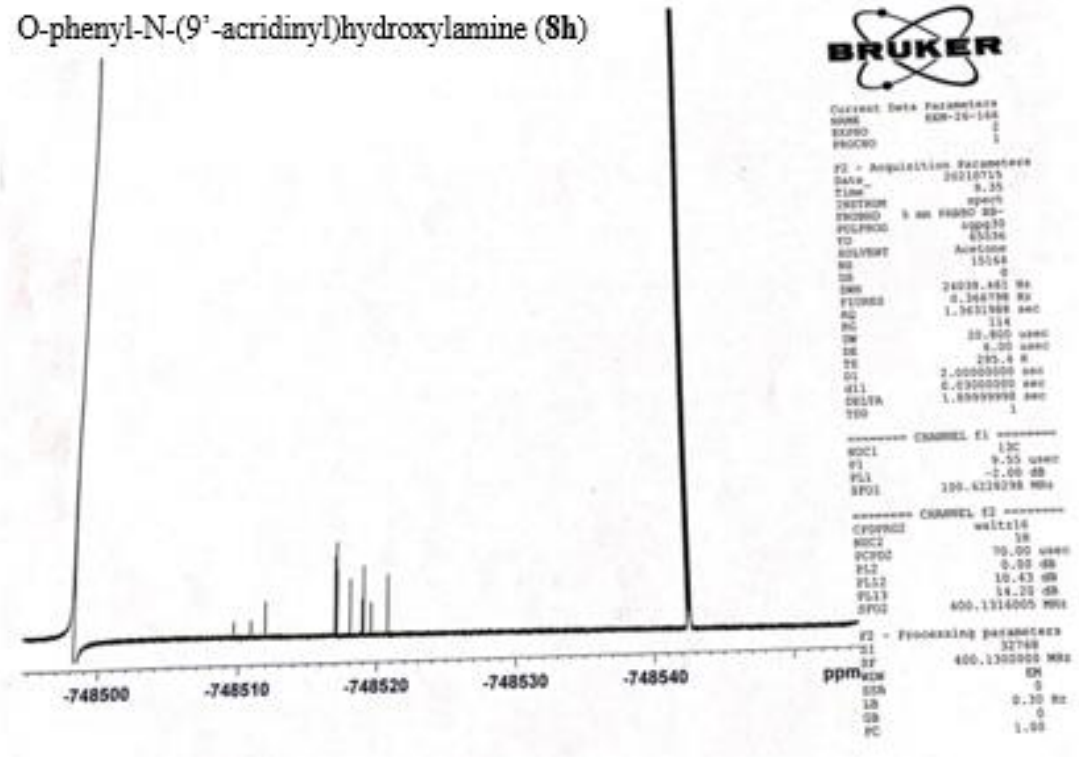

General Procedure for preparation of thermal denaturation analysis

To analyze the O-aryl-N-(9'-acridinyl)hydroxylamines ability to bind to DNA, a solution of compound **8a-h** was prepared to result in a 1:1 molar concentration solution of acridine: DNA. The appropriately substituted O-aryl-N-(9'-acridinyl)hydroxylamine (**8a-h**) was dissolved in 10% DMSO before being combined with the prepared 0.001 M phosphate buffer at pH 6 to make a 1:10 concentration. The DNA solution was made using genomic calf thymus DNA commercially obtained from Sigma Aldrich. A prepared 0.001 phosphate buffer at pH 6 was used to dilute the DNA to a desired volume (10 mL) using a volumetric flask. Absorbance measurements at 258 nm were taken of the DNA solution. The concentration of the DNA solution was calculated using Beer's law with the assumption that $\varepsilon = 5900$ (as a reference). The concentrations of both the DNA and acridine solutions were serial diluted until the desired concentration 1×10^{-6} was obtained. Once the desired concentration was obtained, the two solutions were combined to make 20 mL of a 1:1 molar concentration of acridine: DNA. Thermal denaturation measurements were obtained while the solution was heated at 0.2 °C/minute using the UV-vis. The temperature of the solution was ramped going from 35 to 90 °C. Five trials were conducted for each substituted acridine: DNA solution. The thermal denaturation temperature, T_m, of the DNA in the acridine: DNA solution was determined by plotting the absorbance of the solution at 258 nm versus the increasing temperature.

Figure A.1

Thermal Denaturation Melting Curve for Calf Thymus Deoxyribonucleic Acid Baseline.

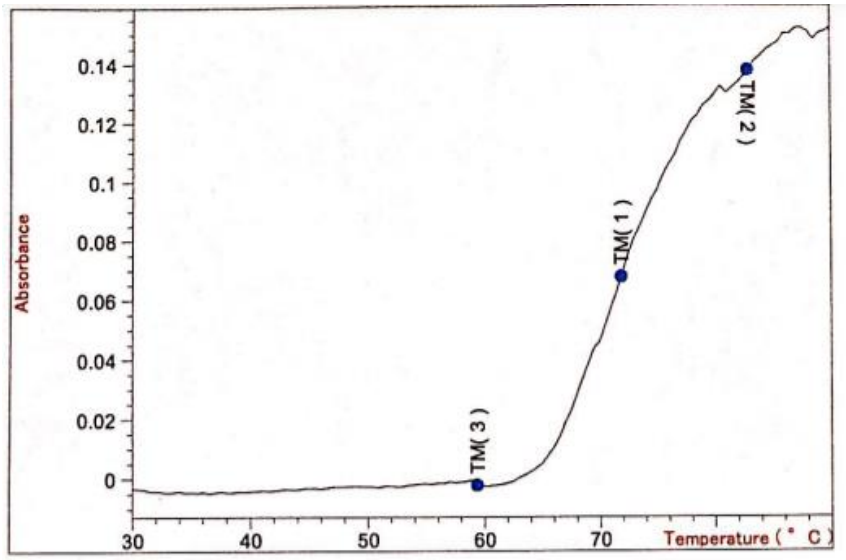

Figure A.2

*Thermal Denaturation Melting Curve for Calf Thymus Deoxyribonucleic Acid: O-(4-methoxyphenyl)-N-(9'-acridinyl)hydroxylamine (**8c**) Solution.*

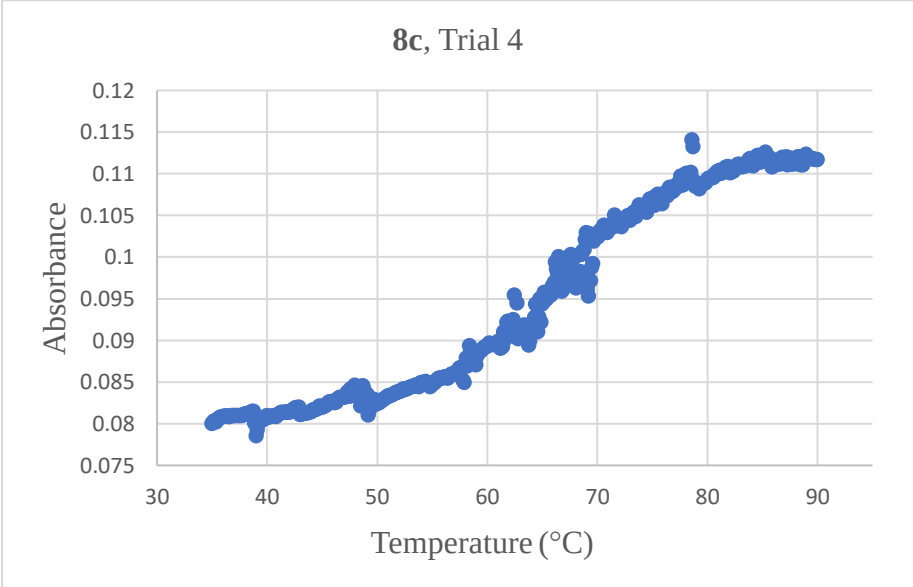

Figure A.3

*Thermal Denaturation Melting Curve for Calf Thymus Deoxyribonucleic Acid: O-Phenyl-N-(9'-acridinyl)hydroxylamine (**8h**) Solution.*